Vacuum stability in the Standard Model with vectorlike fermions

Ash Arsenault,[*] Kivanc Y. Cingiloglu,[†] and Mariana Frank[‡]
Department of Physics, Concordia University, 7141 Sherbrooke Street West, Montreal, Quebec, Canada H4B 1R6

(Received 6 August 2022; accepted 6 February 2023; published 22 February 2023)

The discovery of Standard-Model like Higgs at 125 GeV may raise more questions than the answers it provides. In particular, the hierarchy problem remains unsolved, and the Standard Model Higgs quartic self-coupling becomes negative below the Planck scale, necessitating new physics beyond the Standard Model. In this work we investigate a popular scenario, extensions of the Standard Model with vectorlike fermion fields, such as the ones present in models with extra dimensions or in Higgs composite models, using a model independent approach. Since fermions decrease the Higgs quartic coupling at high energies, only exacerbating the self-coupling problem, we introduce first an additional scalar, which by itself is enough to overcome the vacuum stability limit, and then explore the effects of vectorlike fermions in singlet, doublet and triplet representations. For each model, we identify the allowed fermion masses and mixing angles with the third family fermions required to satisfy the vacuum stability condition, and compare different representations. Allowed fermion masses emerge at around 1 TeV, raising hope that these will be found at the LHC. We also examine corrections to oblique parameters $\mathbb{S}$ and $\mathbb{T}$ from additional scalar and vectorlike quarks which also impose constraints on mixing and mass splitting of both sectors, but these restrictions are relatively weak compared to the vacuum stability.

DOI: 10.1103/PhysRevD.107.036018

I. INTRODUCTION

Ever since the Higgs boson was discovered at the CERN Large Hadron Collider (LHC), confirming at last the last remaining puzzle of the Standard Model (SM) [1], the observed mass of the Higgs boson combined with the mass of the top quark, m_t, have caused concern because, as the theory stands, it violates stability of the electroweak vacuum [2]. In the SM there is a single Higgs h with effective potential characterized by two parameters only, the Higgs $(\text{mass})^2$, κ^2 and its self-coupling λ, $V = \kappa^2 h^2 + \lambda h^4$. The self-coupling λ can become negative at larger scales, so the potential becomes unbounded from below, and there is no resulting stability. Theoretical considerations indicate that if the validity of the SM is extended to M_{Planck}, a second, deeper minimum is located near the Planck scale such that the electroweak vacuum is metastable, i.e., the transition lifetime of the electroweak vacuum to the deeper minimum is finite with lifetime $\sim 10^{300}$ years [2].

If the electroweak vacuum is metastable then Higgs cannot play the role of inflaton [3]. Explanations involving a long lived-universe, where vacuum instability is not important, were proved to be faulty. Without vacuum stability, fluctuations in the Higgs field during inflation and in the hot early universe would have taken most of the universe into an anti–de Sitter phase, yielding a massive collapse, and the expansion of the universe would never have occurred [4]. The result of this is that either the SM must be incorrect or flawed in some way [5], or at the very least, that new physics beyond the SM which alters the Higgs potential so that it enhances its stability must exist at higher energies. Thus extra degrees of freedom are needed for the SM to explain the inflation of the Universe [3,6–8].

Minimal extensions of the SM which stabilize the Higgs vacuum are the most common theories which attempt to solve the Higgs mass problem. The correlation between the Higgs mass and vacuum stability is highly dependent on bosonic interactions. For instance, a model [9] with two Higgs doublets and large soft Higgs mass terms, satisfying the electroweak symmetry breaking conditions, has a stable vacuum and decay branching ratios that are very close to the SM ones, and this only one example.

The question remains if models with additional fermions, present in most beyond the SM scenarios, can survive stability constraints, and if so, what are the restrictions imposed on their masses and mixing (if any) with the SM particles.

[*]ashley.n.arsenault@gmail.com
[†]kivanc.cingiloglu@concordia.ca
[‡]mariana.frank@concordia.ca

To investigate how the hierarchy problem may be fixed, and what are the implications for vacuum stability, one could proceed by assuming a theory which supersedes the SM emerging at higher energies, such a supersymmetry. (Note however that minimal supersymmetry has its own difficulties with accommodating a Higgs boson of mass 125 GeV.) Or one could study the effect of adding particles to the SM, coupled in the simplest way, and investigate the conditions on their masses and couplings as emerging from vacuum stability conditions, as a simple and elegant way to obtain information about new particles and interactions without assuming complicated frameworks.

The latter is the approach we wish to follow in this article, and we investigate inclusion of one additional generation of vectorlike fermions, i.e., fermions whose left-handed and right-handed components transform the same way under $SU(3)_c \times SU(2)_L \times U(1)_Y$. Unlike sequential fourth-generation quarks, which are ruled out by the one-loop induced Higgs production and decay mechanisms (the gluon fusion production and diphoton decay of the Higgs) [10], indirect bounds on vectorlike quarks are much weaker. In particular, vectorlike fermions can acquire a large Dirac mass without introducing a large Yukawa coupling to the Higgs.

Vectorlike fermions appear in the context of many models of New Physics [11]. In warped or universal extra dimensional models, vectorlike fermions appear as KK excitations of bulk fields [12], in Composite Higgs models, vectorlike quarks emerge as excited resonances of bound states that form SM particles [13,14], in little Higgs models, they are partners of the ordinary fermions within larger group representations and charged under the group [15], and in nonminimal supersymmetric extensions of the SM, they can increase the Higgs mass through loop corrections without adversely affecting electroweak precision [16]. Vectorlike colored particles are consistent with perturbative gauge coupling unification and are often invoked to explain discrepancies in the data, such as the $t\bar{t}H$ anomaly [17].

Vectorlike particles have been considered before in the context of stabilizing the vacuum of the SM in [18,19], in the context of baryogenesis [20], to account for the anomalous magnetic moment of the muon and discrepancies in the W boson mass [21], and to help explain the observed excess at 750 GeV [22,23]. However, only particular representations have been considered [24], and a complete interplay of all possible vectorlike quark representations and the SM does not exist at present. We redress this here, and analyze the restrictions on the masses and mixing angles for the all anomaly-free representations of vectorlike quarks, as well as the associated boson field which is added to the SM for vacuum stabilization. In addition, we test the effects and restrictions induced by the vectorlike fermions on the electroweak precision observables, $\mathbb{S}, \mathbb{T}$, and $\mathbb{U}$.

Our work is organized as follows. In Sec. II we outline briefly the vacuum stability problem in the SM, and in Sec. II B its resolution with an additional singlet scalar. In Sec. III we then introduce all anomaly-free vectorlike quark representations, their interaction Lagrangians, and derive their masses and mixing angles (assumed to be with the third generation quarks only). We then proceed to analyze the effects on vacuum stability of introducing singlet, doublet, and triplet representations, respectively. In Sec. IV we give the expressions and analyze the effects of the additional fields on the electroweak precision observables. We conclude in Sec. V, and leave the expressions for the relevant RGEs for the models studied to the Appendix.

II. VACUUM STABILITY IN THE SM

A. The Higgs potential

In the SM, interactions with the Higgs field are specified by the Higgs potential, which has the form

$$V(\phi) = -\frac{1}{2}\kappa^2\Phi^2 + \frac{1}{4}\lambda\Phi^4 + \Delta V, \tag{2.1}$$

with κ and λ the quadratic and quartic couplings, ΔV the tree-level correction terms, and Φ the Higgs field given by

$$\Phi = \begin{pmatrix} \Phi^+ \\ \Phi^0 \end{pmatrix} = \begin{pmatrix} \Phi^+ \\ (v + h^0 + iG^0)/\sqrt{2} \end{pmatrix}, \tag{2.2}$$

where $v = 246$ GeV is the Higgs vacuum expectation value (VEV). Vacuum stability requires $V'(\phi) > 0$, or equivalently, $\lambda(\mu) > 0$, with λ the running Higgs coupling which depends on the scale, μ, at which the SM breaks down. The issue is that the Higgs quadratic self-coupling is renormalized not only by itself (λ increasing as the energy scale increases), but also by the Higgs (Yukawa) coupling to the top quark, which tends to drive it to smaller, even negative values at high scales μ. At leading orders [25]

$$\lambda(\mu) \simeq \lambda(\mu_0) - \frac{3m_t^2}{2\pi v^4}\log\left(\frac{\mu}{\mu_0}\right), \tag{2.3}$$

yielding an estimate for the energy scale where λ will become negative [25]

$$\log\left(\frac{\mu}{\mu_0}\right) = 9.4 + 0.7(m_H - 125.15) - 1.0(m_t - 173.34) + 0.3\left(\frac{\alpha_s(M_Z) - 0.1184}{0.0007}\right) \tag{2.4}$$

with energy scales and masses measured in GeV. Taking into account all the uncertainties in the measurements of m_H, m_t, and α_s, the scale at which the SM fails is

$\mu = 10^{(9.4\pm1.1)}$ GeV. Possible remedies include higher-dimensional operators in the effective theory, or additional symmetries (such as supersymmetry, which is associated to a new scale), or addition of new particles to the SM.

More explicitly, the variation of the coupling λ with the energy scale involves evaluation of the one-loop beta function describing the running of λ is [25]

$$\frac{d\lambda(\mu)}{d\ln\mu} = \frac{1}{16\pi^2}\left[4\lambda^2 + 12\lambda y_t^2 - 36y_t^2 - 9\lambda g_1^2 - 3\lambda g_2^2 + \frac{9}{4}g_2^2 + \frac{9}{2}g_1^2 g_2^2 + \frac{27}{4}g_1^4\right], \tag{2.5}$$

with g_1, g_2, g_3 the coupling constants for $U(1)_Y, SU(2)_L$, $SU(3)_c$, and y_t the Yukawa coupling of the top quark. The renormalization group equations for these parameters are [26]

$$\frac{dg_i(\mu)}{d\ln\mu} = \frac{1}{16\pi^2}b_i g_i^3, \qquad b = (41/10, -19/6, -7) \tag{2.6}$$

$$\frac{dy_t(\mu)}{d\ln\mu} = \frac{y_t}{16\pi^2}\left[\frac{9}{2}y_t^2 - \frac{9}{4}g_2^2 - \frac{17}{12}g_1^2 - 8g_3^2\right], \tag{2.7}$$

with initial conditions

$$g_1^2(\mu_0) = 4\pi\alpha, \qquad g_2^2(\mu_0) = 4\pi\alpha\left(\frac{1}{\sin\theta_W} + 1\right), \qquad g_3^2(\mu_0) = 4\pi\alpha_s$$
$$y_t(\mu_0) = \frac{\sqrt{2}m_t}{v}, \qquad \lambda(\mu_0) = \frac{3m_H^2}{v^2}[1 + \delta_\lambda(\mu_0)]. \tag{2.8}$$

Here α, α_s are the weak and strong coupling constants, $\sin\theta_W = 0.2312$ is the Weinberg angle, and we set $\mu_0 = M_Z = 91.188$ GeV. The radiative decay constant is [27]

$$\delta_\lambda(\mu) = \frac{G_F M_Z^2}{8\sqrt{2}\pi^2}[\xi f_1(\xi,\mu) + f_0(\xi,\mu) + \xi^{-1}f_{-1}(\xi,\mu)], \tag{2.9}$$

with $\xi = m_H^2/M_Z^2$, $G_F = 1.16635 \times 10^{-5}$ GeV^{-2} and

$$f_1(\xi,\mu) = 6\ln\frac{\mu^2}{m_H^2} + \frac{3}{2}\ln\xi - \frac{1}{2}Z\left(\frac{1}{\xi}\right) - Z\left(\frac{c^2}{\xi}\right) - \ln c^2 + \frac{9}{2}\left(\frac{25}{9} - \sqrt{\frac{1}{3}}\pi\right)$$
$$f_0(\xi,\mu) = 6\ln\frac{\mu^2}{M_Z^2}\left[1 + 2c^2 - 2\frac{m_t^2}{M_Z^2}\right] + \frac{3c^2\xi}{\xi - c^2} + 2Z\left(\frac{1}{\xi}\right) + 4c^2 Z\left(\frac{c^2}{\xi}\right) + \frac{3c^2\ln c^2}{s^2} + 12c^2\ln c^2 - \frac{15}{2}(1 + 2c^2)$$
$$- 3\frac{m_t^2}{M_Z^2}\left[2Z\left(\frac{m_t^2}{\xi M_Z^2}\right) + 4\ln\frac{m_t^2}{M_Z^2} - 5\right],$$
$$f_{-1}(\xi,\mu) = 6\ln\frac{\mu^2}{M_Z^2}\left[1 + 2c^4 - 24\frac{m_t^2}{M_Z^2}\right] - 6Z\left(\frac{1}{\xi}\right) - 12c^4 Z\left(\frac{c^2}{\xi}\right) - 12c^4\ln c^2 + 8(1 + 2c^4) + \left[Z\left(\frac{m_t^2}{\xi M_Z^2}\right) + \ln\frac{m_t^2}{M_Z^2} - 2\right] \tag{2.10}$$

with

$$Z(z) = \begin{cases} 2A\tan^{-1}(1/A), & z > 1/4 \\ A\ln[(1+A)/(1-A)], & z < 1/4, \end{cases} \tag{2.11}$$

$$A = |1 - 4z|^1/2 \tag{2.12}$$

where c, s are abbreviations for $\cos\theta_W, \sin\theta_W$.

Examining the running of the coupling parameters in this mode shows that the scalar couplings increase with increasing energy scales, while the Higgs coupling λ decreases and becomes negative at around 10^{10} GeV.

B. Introducing an additional boson

In this section, we consider the simplest remedy to the stability problem by extending the particle content of the SM by an extra (singlet, as it is simplest) scalar boson which interacts solely with the SM Higgs, and we examine the constraints placed on its mass and its mixing angle with the SM Higgs boson on experimental and theoretical grounds. We leave Higgs vacuum stability condition, the main motivations of this work, to be analyzed in detail in the last discussion in this section. We refer to this scenario as HSM.

The addition of a boson provides a positive boost to the coupling parameter, counteracting the effect of the top

quark and contributing toward repairing the Higgs vacuum stability [28].

In this scenario, the Higgs doublet Φ from Eq. (2.2) interacts with the new scalar singlet χ

$$\chi = (u + \chi^0), \tag{2.13}$$

where u is the singlet VEV, through

$$V(\phi,\chi) = -\kappa_H^2\Phi^\dagger\Phi + \lambda_H(\Phi^\dagger\Phi)^2 - \frac{\kappa_S^2}{2}\chi^2 + \frac{\lambda_S}{4}\chi^4 + \frac{\lambda_{SH}}{2}(\Phi^\dagger\Phi)^2\chi^2. \tag{2.14}$$

After symmetry breaking, the singlet and doublet Higgs mix

$$\mathcal{M}_{H,S} = \begin{pmatrix} 2\lambda_H v^2 & \lambda_{SH} vu \\ \lambda_{SH} vu & 2\lambda_S u^2 \end{pmatrix}, \tag{2.15}$$

yielding mass eigenvalues:

$$m^2_{H,S} = \lambda_H v^2 + \lambda_S u^2 \mp \sqrt{(\lambda_S u^2 - \lambda_H v^2)^2 + \lambda^2_{SH} u^2 v^2} \tag{2.16}$$

and the eigenvectors

$$\begin{pmatrix} H \\ S \end{pmatrix} = \begin{pmatrix} \cos\varphi & \sin\varphi \\ -\sin\varphi & \cos\varphi \end{pmatrix}\begin{pmatrix} \Phi \\ \chi \end{pmatrix}. \tag{2.17}$$

As in the SM, we require $\lambda_H > 0$ for a stable SM vacuum, and $\lambda_S > 0$ for the new particle. In addition we impose that the potential is positive for asymptotically large values of the fields,

$$\lambda_H > 0, \qquad 0 < \lambda_S < 4\pi, \qquad |\lambda_{SH}| > -2\sqrt{\lambda_S\lambda_H}. \tag{2.18}$$

In addition we require that λ_{SH} is perturbative, thus bounded by $|\lambda_{SH}| > 4\pi$. The quartic couplings can be expressed in terms of the physical masses as:

$$\begin{aligned} \lambda_H &= \frac{m_H^2\cos^2\varphi + m_S^2\sin^2\varphi}{2v^2}, \\ \lambda_S &= \frac{m_S^2\cos^2\varphi + m_H^2\sin^2\varphi}{2v^2}, \\ \lambda_{SH} &= \frac{m_S^2 - m_H^2}{2uv}\sin 2\varphi, \end{aligned} \tag{2.19}$$

with $m_H, m_S(v,u)$ the masses (VEVs) of the physical fields, respectively and φ their mixing angle. Requiring perturbativity up to Planck scales, we apply the Yukawa and Higgs sector RGEs:

$$\begin{aligned} \frac{dy_t^2}{d\ln\mu^2} &= \frac{y_t^2}{16\pi^2}\left(\frac{9y_t^2}{2} - \frac{17g_1^2}{20} - \frac{9g_2^2}{4} - 8g_3^2\right), \\ \frac{d\lambda_H}{d\ln\mu^2} &= \frac{1}{16\pi^2}\left[\lambda_H\left(12\lambda_H + 6y_t^2 - \frac{9g_1^2}{10} - \frac{9g_2^2}{2}\right) + \left(\frac{\lambda_{SH}^2}{4} - 3y_t^4 + \frac{27g_1^4}{400} + \frac{9g_2^4}{16} + \frac{9g_1^2g_2^2}{40}\right)\right], \\ \frac{d\lambda_S}{d\ln\mu^2} &= \frac{1}{16\pi^2}(9\lambda_S^2 + \lambda_{SH}^2), \\ \frac{d\lambda_{SH}}{d\ln\mu^2} &= \frac{\lambda_{SH}}{16\pi^2}\left(2\lambda_{SH} + 6\lambda_H + 3\lambda_S + 3\lambda_S + 3y_t^2 - \frac{9g_1^2}{20} - \frac{9g_2^2}{4}\right), \end{aligned} \tag{2.20}$$

Here λ_H and λ_S are the quartic self-couplings of Φ and χ, and λ_{SH} the coupling describing their mixing. Equation (2.19) describe the coupling parameters at relatively small energy scales, and therefore serve as initial conditions to these RGEs.

Just as in the SM, we ignore the contributions of all Yukawa couplings except for that of the top quark, and also, we include electroweak radiative correction terms for increased accuracy. To this end, we replace the top Yukawa coupling and Higgs self-coupling boundary conditions with [29]

$$\begin{aligned} y_t &= \frac{\sqrt{2}m_t}{v}[1 + \Delta_t(\mu_0)], \\ \lambda_H &= \frac{m_H^2\cos^2\varphi + m_S^2\sin^2\varphi}{2v^2}[1 + \Delta_H(\mu_0)], \end{aligned} \tag{2.21}$$

where $\Delta_H(\mu)$ is the same correction as in the SM, and

$$\Delta_t(\mu_0) = \Delta_W(\mu_0) + \Delta_{\mathrm{QED}}(\mu_0) + \Delta_{\mathrm{QCD}}(\mu_0), \tag{2.22}$$

with

$$\Delta_W(\mu_0) = \frac{G_F m_t^2}{16\sqrt{2}\pi^2}\left(-9\ln\frac{m_t^2}{\mu_0^2} - 4\pi\frac{m_H}{m_t} + 11\right),$$
$$\Delta_{\rm QED}(\mu_0) = \frac{\alpha}{9\pi}\left(3\ln\frac{m_t^2}{\mu_0^2} - 4\right),$$
$$\Delta_{\rm QCD}(\mu_0) = \frac{\alpha_s}{9\pi}\left(3\ln\frac{m_t^2}{\mu_0^2} - 4\right), \quad (2.23)$$

and we include the RGEs for the gauge couplings as in the SM, Eq. (2.6).

Figure 1 illustrates the running of the coupling parameters for a typical set of parameter values. Notice that in this model, the scalar couplings increase with increasing energy scales, compensating for the SM Higgs coupling, which becomes negative at around 10^{10} GeV. Therefore, the addition of an extra scalar boson to the SM rescues the theory from vacuum instability. Of course, we may investigate the mass and mixing angle of this singlet scalar with the Higgs boson by eliminating all parameter values that do not satisfy Higgs vacuum stability. For this we perform a scan over a broad parameter space and disallow all parameter values which do not satisfy the vacuum stability conditions outlined in Eq. (2.18). The resulting allowed parameter space is illustrated in Fig. 2. While the blue points represent restrictions from vacuum stability bounds only, the shaded red region represents the region excluded by constraints from Higgs production and couplings (as discussed below), which are dominant and are the only parameters limiting the parameter space, especially for lighter singlet masses, $m_S \leq 700$ GeV.

Note that, while the mass region allowed for the additional boson for $u = 1$ TeV is quite restricted, for larger VEVs it is quite large, and increasing with the new boson VEV. However, in all cases, the mixing with the SM Higgs boson is required to be nonzero ($\varphi \neq 0$), consistent with the observation of Higgs potential instability in the absence of the additional boson.

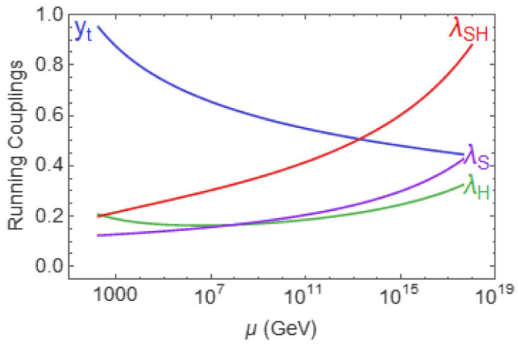

FIG. 1. The RGE running of the top Yukawa coupling and scalar couplings for the scalar boson model with $m_S = 1$ TeV, $\sin\varphi = 0.1$, $u = 2$ TeV, and setting the starting point of the running at $\mu_0 = m_t$.

The additional scalar is subjected to constraints from particle physics and cosmology [30,31]. If the additional scalar is heavier than the Higgs boson at 125 GeV, in HSM the decay channel $S \to HH$ may exist, and act as an extra constraint for the mixing regime. The ρ parameter and its deviation from unity play an important role in measuring the effects of new physics on the masses of electroweak gauge bosons. Corrections to the mass of W-boson originate from the Higgs mediated loops, which enhance gauge boson self-energies, and these are dependent on the masses and the mixing between the scalar fields [32]. In the case where the heavier of the two scalars is the mostly singlet S with $m_S \geq 125$ GeV, the mixing angle $\sin\varphi$ agrees with theoretical predictions up to 1σ. Although the region for ΔM_W [1] is less restricted compared to the other case (where $m_H = 125$ GeV), this scenario is disfavored by collider bounds and Higgs data. If the lighter scalar corresponds to the SM Higgs boson with $m_H = 125$ GeV, larger heavy singlet scalar masses impose smaller mixing angles between the two scalars in order to fit ΔM_W to 1σ level. The minimum scale for the mass of heavier scalar in this work is at least 500 GeV, which in return, corresponds to $\sin\varphi = 0.37$ due only to the constraint on ΔM_W.

The bounds on HSM are also constrained by electroweak precision observables (EWPO). The singlet scalar contributes to the gauge boson self-energy diagrams at loop level, generating a shift in the oblique parameters S, T, U [34]. Checking the results from EWPO fit [35] by taking into account only the deviation of the oblique parameters with respect to the SM [33], Fig. 3 shows that, for values of m_S below 1 TeV, the restrictions from the bounds from Higgs signal strength are stronger than those from EWPO. For the case considered in this work, where $m_S \leq 2$ TeV, the parameter space corresponding to agreement between oblique parameters and the EWPO fit imposes an upper bound for $\sin\varphi < 0.4$ around $m_S = 500$ GeV. The effects arising from electroweak precision in HSM, at 1σ level [32] are consistent with our later considerations of S, T, U parameters in Sec. IV which indicate that, for mass of the singlet Higgs at 1 TeV, the mixing angle must be $\sin\varphi < 0.2$ from the requirement of consistency of new physics with allowed deviations from the SM. These results are consistent with those in Fig. 2.

An additional theoretical bound comes from perturbative unitary. Two body scattering of scalars at tree level and loop effects to the partial decay widths were derived for HSM in [36]. Near the decoupling region $\sin\varphi \sim 0$, unitarity alone puts a lower bound for $m_S \geq 1$ TeV to one-loop level, whereas otherwise m_S can be as large as 7 TeV. In addition,

[1]Please note that in this work we assumed $M_W = 80.377 \pm 0.012$ GeV [33] and did not take into account the new CDF measurement, awaiting further confirmation. Our results are thus more conservative.

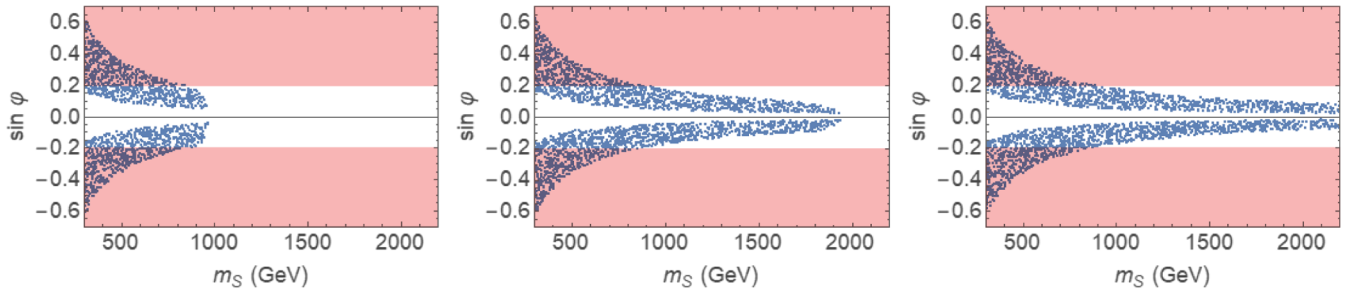

(a) $u = 1$ TeV. (b) $u = 2$ TeV. (c) $u = 4$ TeV.

FIG. 2. The allowed parameter space for the mass m_S and mixing angle φ with the SM Higgs for the additional scalar boson model, for different vacuum expectation values: $u = 1$ TeV (a); $u = 2$ TeV (b); and $u = 4$ TeV (c). The shaded region represents the region excluded by constraints from the Higgs data.

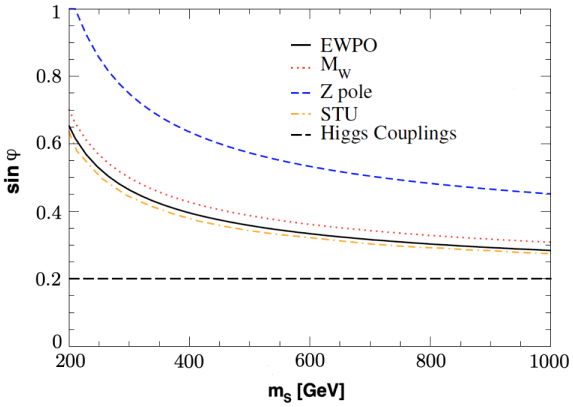

FIG. 3. Allowed parameter space for the singlet scalar mass m_S and the maximum value of the mixing angle $\sin\varphi$ in HSM with respect to various constraints in HSM.

a lower bound rising from unitarity can be computed at tree level according to the mixing relation

$$m_S^2 \sin\varphi^2 + m_H^2 \cos\varphi^2 \geq \frac{4\pi\sqrt{2}}{3G_F} \simeq 700\ \text{GeV}^2 \qquad (2.24)$$

But in general, perturbative unitarity generates a more flexible parameter space compared to other constraints.

The Higgs singlet also affects signal rates due to loop effects on the Higgs decay widths through the channels $H \to gg, \gamma\gamma$ at leading order. Previous analyses used various benchmark to test behaviors for different $\tan\beta$, defined as the ratio of the VEVs $\tan\beta = \frac{u}{v}$, and m_S scales [37]. The mixing between scalars ranges in the interval $\sin\varphi = (0.31 - 0.20)$, corresponding to $m_S = (200\text{–}800\ \text{GeV})$. The parameter space generated from the additional Higgs production channel $S \to HH$ is in agreement with $H \to$ diboson decays for $\sin\varphi \leq 0.22$ in the mass range $m_S = (260\text{–}770\ \text{GeV})$, corresponding to the minimum of $\text{BR}(S \to HH) = 0.17$. The mixing is further constrained with increasing mass values of the Higgs singlet, $\sin\varphi \leq 0.16$, for $m_S \leq 1$ TeV [38].

Apart from the SM Higgs quartic coupling λ_H, the couplings λ_S and λ_{HS} from Eq. (2.14) are inversely proportional to $\tan\beta$, which yields $\lambda_i > 1$ at $\tan\beta \sim 1$, $m_S \geq 900$ GeV. So, λ_S and λ_{HS} reach the nonperturbativity region for small $\tan\beta$ values. Taking relatively larger VEV scales, the couplings are perturbative for $\tan\beta = 5$, 10,

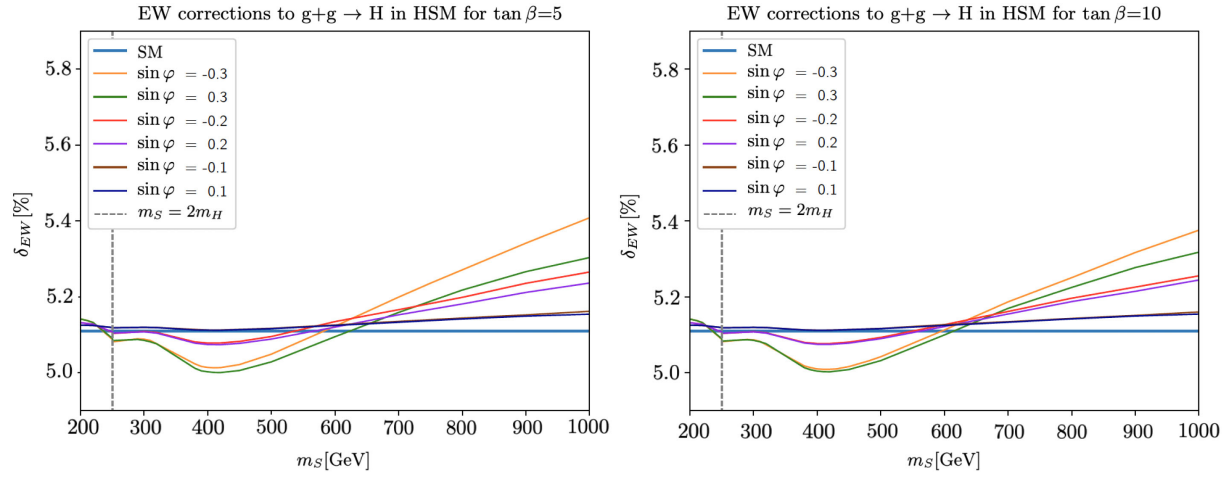

FIG. 4. Electroweak corrections δ_{EW} to leading order of cross section of SM Higgs production via gluon fusion in HSM for different VEV ratios, $\tan\beta = \frac{u}{v} = 5$, 10, as a function of the additional singlet mass.

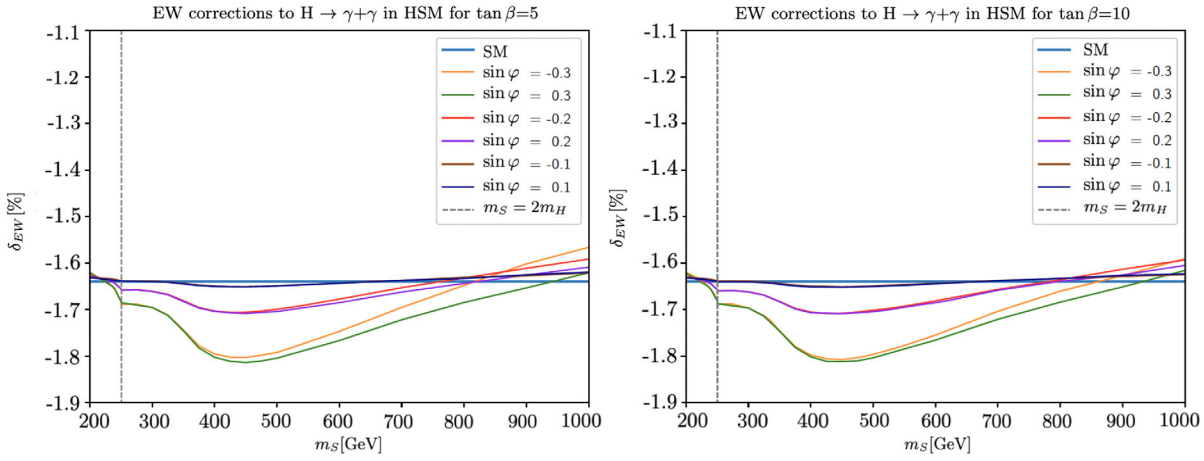

FIG. 5. Electroweak corrections δ_{EW} to the partial decay width of the diphoton decay $H \to \gamma\gamma$ in HSM for different VEV ratios, $\tan\beta = \frac{u}{v} = 5$, 10, as a function of the additional singlet mass.

which correspond to the singlet VEV scales, $u = 1$, 2 TeV throughout our work. Figure 4 shows the electroweak corrections to the production $gg \to H$ while Fig. 5 shows the decay $H \to \gamma\gamma$, indicating that the electroweak correction δ_{EW} becomes more consistent with the SM limit (blue line) as $\tan\beta$ becomes larger. For $\tan\beta = 10$, $u \sim 2$ TeV, δ_{EW} further tends to the SM scale, however, variations in $\sin\varphi$ become $\tan\beta$ suppressed.

Figure II B yields a strong constraint on the scalar mixing, because for electroweak deviations δ_{EW} to converge toward the SM limit, $\sin\varphi \leq |0.2|$ at TeV scale. Electroweak constraints are more relaxed from diphoton decay Fig. 5. Deviations from the SM are not too severe on $\sin\varphi$ when $m_S \geq 800$ GeV. Clearly, as $\tan\beta$ becomes larger (and so does the singlet VEV u), the constraints obtained from $H \to$ diboson channels are satisfied for $m_S = \mathcal{O}(\mathrm{TeV})$ scale. On the other hand, the region with small $\tan\beta$ in HSM is restricted from perturbativity and relatively larger δ_{EW} inconsistencies.

The production and decay channels of the singlet scalar are shown in Figs. 6 and 7, respectively. The processes $gg \to S$ and $S \to \gamma\gamma$ have no useful experimental bounds for extracting various constraints on HSM. However the corrections δ_{EW} are more dependent on the sign of $\sin\varphi$ than on $\tan\beta$. Similarly, smaller β values restrict the perturbativity of λ_S and λ_{HS} for $m_S \geq 900$ GeV.

Cosmological constraints on models with additional scalars are interested particularly in cases where the additional singlet is a dark matter candidate. Among the Higgs related dark matter (DM) portal studies, only the scalar portal is renormalizable. However, when it comes to scalar portals, the coupling between different scalars can take values in a relatively large interval. In HSM, λ_{HS} sets various constraints on the freezing temperature T_f at which DM decouples from cosmic heat reservoir [39]. Although additional DM candidates such as singlet fermions can be added to any theory in order to decrease extremely divergent

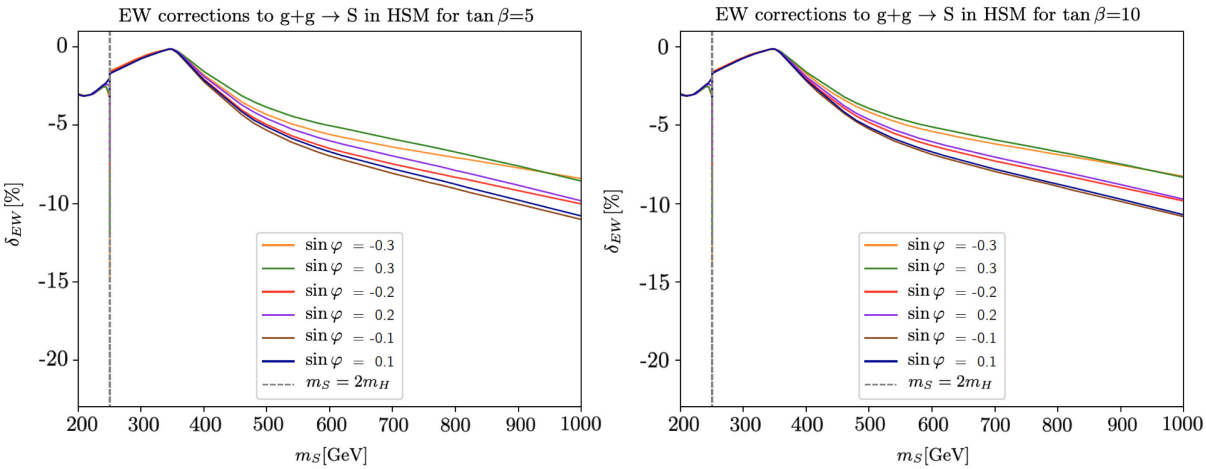

FIG. 6. Electroweak corrections δ_{EW} to leading order of cross section of the singlet Higgs production via gluon fusion in HSM for different VEV ratios, $\tan\beta = \frac{u}{v} = 5$, 10, as a function of the singlet mass.

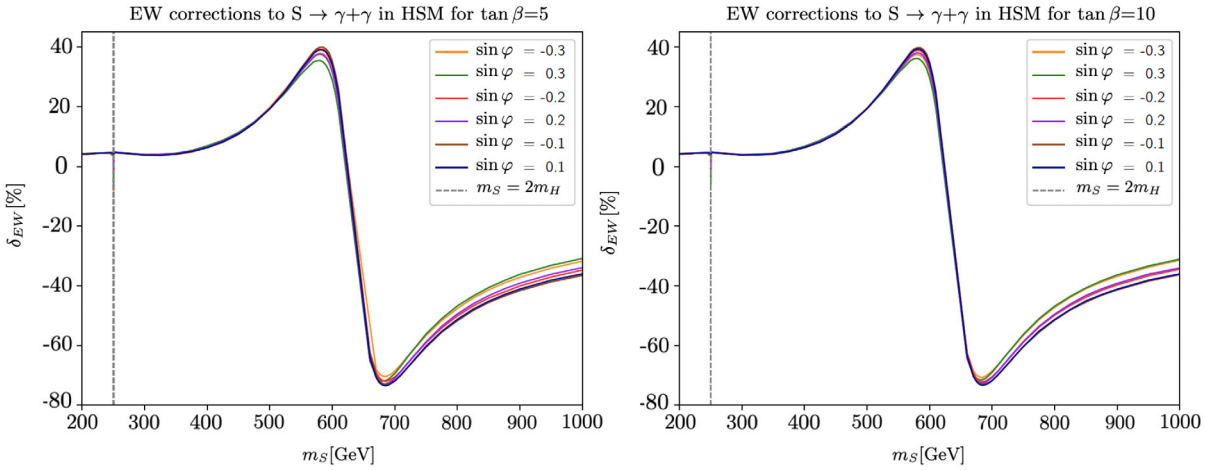

FIG. 7. Electroweak corrections δ_{EW} to leading order of the partial decay width of the diphoton decay $S \to \gamma\gamma$ (bottom panel) in HSM for different VEV ratios, $\tan\beta = \frac{u}{v} = 5$, 10, as a function of the singlet mass.

characteristic of λ_{HS} in RGE level, mixing constraints are still in agreement with other constraints; $m_S < 1$ TeV (without extra fermionic DM), and $200 < m_S < 300$ GeV (with extra fermionic DM) as the Universe cools down $T < T_f$ [40]. Furthermore, if the singlet VEV $u < 400$ GeV, $\tan\beta < 2$ in order to allow perturbativity of λ_{HS}; this is however outside the parameter region we considered. Electroweak vacuum stability is affected by the renormalization group equations for the coupling of λ_H to λ_{HS} in Eq. (2.20), hence the connection between coupling evolutions gives limited freedom to control the dependence of λ_{HS} on m_S. The combined cosmological constraints were explored within the GAMBIT framework [41], and they concluded that for $1 < m_S < 4$ TeV the singlet scalar portal only can account for the relic abundance. A more recent work [42] treats the electroweak stability problem by analyzing the HSM potential and transition probability of VEVs through radiation dominated era by an transcendental function of temperature. In accordance with the results of this work [42], m_S might have to extend to TeV scale to have a stable vacuum, though the exact lower value of m_S depends on the scale of λ_{HS}.

Overall, our explored parameter space of SM with the additional scalar is consistent with Higgs data, electroweak constraints, and cosmological constraints. We showed that regions with singlet masses and VEVs around the TeV scale are much preferred. We now proceed to analyze the effects of introducing vectorlike quarks to the model and show that there, as we add more fermions, stability emerges be the most stringent constraint.

III. VACUUM STABILITY IN THE SM WITH VECTORLIKE FERMIONS

A. Theoretical considerations

Using the stable potential in the previous section, we investigate the effect of introducing vectorlike fermions into this SM + additional scalar model. Unlike SM-like (chiral) fermions which act as doublets under $SU(2)_L$ if left-handed and as singlets if right-handed, and spoil the agreement of loop-induced production and decays of the SM Higgs, vectorlike fermions have the same interactions regardless of chirality. They appear in many new physics models, such as models with extra dimensions, and many explanations put forward of deviations from SM physics include vectorlike fermions. Thus it is important that, when considering the addition of a vectorlike fermions to the SM, the presence of a new scalar boson is essential to ensure the stability of the Higgs potential, otherwise, as the fermions decrease the effective self coupling, the singular divergence of the Higgs quartic coupling would worsen compared to the one in the SM. As before we require the Higgs sector potential to be positive at asymptotically large values of the fields, up to Planck scale. The question we need to address is: what are the constraints on the masses of the vectorlike fermions, and mixing angles with ordinary fermions, such as to maintain vacuum stability.

The new states interact with the Higgs bosons through Yukawa interactions. The allowed anomaly-free multiplet states for the vectorlike quarks, together with their nomenclature, are listed in Table I [11,24,43]. The first two representations are U-like and D-like singlets, the next three are doublets (one SM-like, two non-SM like), and the

TABLE I. Representations of vectorlike quarks, with quantum numbers under $SU(2)_L \times U(1)_Y$.

Name	$\mathcal{U}_1$	$\mathcal{D}_1$	$\mathcal{D}_2$	$\mathcal{D}_X$	$\mathcal{D}_Y$	$\mathcal{T}_X$	$\mathcal{T}_Y$
Type	Singlet	Singlet	Doublet	Doublet	Doublet	Triplet	Triplet
	T	B	$\begin{pmatrix} T \\ B \end{pmatrix}$	$\begin{pmatrix} X \\ T \end{pmatrix}$	$\begin{pmatrix} B \\ Y \end{pmatrix}$	$\begin{pmatrix} X \\ T \\ B \end{pmatrix}$	$\begin{pmatrix} T \\ B \\ Y \end{pmatrix}$
$SU(2)_L$	1	1	2	2	2	3	3
Y	2/3	−1/3	1/6	7/6	−5/6	2/3	−1/3

last two are triplets. The various representations are distinguished by their $SU(2)_L$ and hypercharge numbers. In these representations, the Yukawa and the relevant interaction terms between the vectorlike quarks and SM quarks are, in the mixed (H, S) basis

$$\begin{aligned}
\mathcal{L}_{SM+S} &= -y_u \bar{q}_L H^c u_R - y_d \bar{q}_L H d_R \\
\mathcal{L}_{\mathcal{U}_1,\mathcal{D}_1} &= -y_T \bar{q}_L H^c U_{1_R} - y_B \bar{q}_L H D_{1_R} - y_M(\bar{U}_{1_L} S U_{1_R} + \bar{D}_{1_L} S D_{1_R}) - M_U \bar{U}_L U_R - M_D \bar{D}_L D_R, \\
\mathcal{L}_{\mathcal{D}_2} &= -y_T \bar{D}_{2_L} H^c u_R - y_B \bar{D}_{2_L} H d_R - y_M(\bar{D}_{2_L} S^c D_{2_R} + y_B \bar{D}_{2_L} S D_{2_R}) - M_D \bar{D}_{2_L} D_{2_R}, \\
\mathcal{L}_{\mathcal{D}_X,\mathcal{D}_Y} &= -y_T \bar{D}_{X_L} H u_R - y_B \bar{D}_{Y_L} H^c d_R - y_M(\bar{D}_{X_L} S D_{X_R} + y_B \bar{D}_{Y_L} S^c D_{Y_R}) - M_X \bar{D}_{X_L} D_{X_R} - M_Y \bar{D}_{Y_L} D_{Y_R}, \\
\mathcal{L}_{\mathcal{T}_X,\mathcal{T}_Y} &= -y_T \bar{q}_L \tau^a H^c \mathcal{T}^a_{X_R} - y_B \bar{q}_L \tau^a H \mathcal{T}^a_{Y_R} - y_M(\bar{\mathcal{T}}_{X_L} \tau^a S^c \mathcal{T}^a_{X_R} + y_B \bar{\mathcal{T}}_{Y_L} \tau^a S \mathcal{T}^a_{Y_R}) - M_X \bar{\mathcal{T}}_{X_L} \mathcal{T}_{X_R} - M_Y \bar{\mathcal{T}}_{Y_L} \mathcal{T}_{Y_R},
\end{aligned} \tag{3.1}$$

where $H^c = i\sigma^2 H^\star$, $S^c = i\sigma^2 S$, y_u, y_d, y_T, and y_B and the Yukawa couplings of the SM-like Higgs field H, and y_M is the Yukawa coupling of the S field to vectorlike quarks. After spontaneous symmetry breaking, the Yukawa interactions generate mixing between the SM quarks and the vectorlike quarks at tree level. The singlet vectorlike quark and the triplet vectorlike quark exhibit similar mixing patterns, while the doublet vectorlike quarks have a different mixing pattern. To avoid conflicts with low energy experimental data (flavor changing neutral interactions), we limit the vectorlike quarks mixing with the third generation of SM quarks only. This is reasonable also because of the large mass gap between vectorlike fermions and the first two generations of quarks. The mixing patterns will be described below.

The gauge eigenstate fields resulting from the mixing can be written in general as,

$$\mathcal{T}_{L,R} = \begin{pmatrix} t \\ T \end{pmatrix}_{L,R} \qquad \mathcal{B}_{L,R} = \begin{pmatrix} b \\ B \end{pmatrix}_{L,R} \tag{3.2}$$

The mass eigenstate fields are denoted as (t_1, t_2) and (b_1, b_2) and they are found through biunitary transformations,

$$\begin{aligned}
\mathbf{T}_{L,R} &= \begin{pmatrix} t_1 \\ t_2 \end{pmatrix}_{L,R} = V^t_{L,R} \begin{pmatrix} t \\ T \end{pmatrix}_{L,R} \\
\mathbf{B}_{L,R} &= \begin{pmatrix} b_1 \\ b_2 \end{pmatrix}_{L,R} = V^b_{L,R} \begin{pmatrix} b \\ B \end{pmatrix}_{L,R},
\end{aligned} \tag{3.3}$$

where

$$\begin{aligned}
V^t_{L,R} &= \begin{pmatrix} \cos\theta & -\sin\theta \\ \sin\theta & \cos\theta \end{pmatrix}_{L,R}, \\
V^b_{L,R} &= \begin{pmatrix} \cos\beta & -\sin\beta \\ \sin\beta & \cos\beta \end{pmatrix}_{L,R},
\end{aligned} \tag{3.4}$$

In the following we abbreviate $\cos\theta^t_L \equiv c^t_L$, ... Through these rotations we obtain the diagonal mass matrices

$$\begin{aligned}
M^t_{\text{diag}} &= V^t_L M^t (V^t_R)^\dagger = \begin{pmatrix} m_{t_1} & 0 \\ 0 & m_{t_2} \end{pmatrix}, \\
M^b_{\text{diag}} &= V^b_L M^b (V^b_R)^\dagger = \begin{pmatrix} m_{b_1} & 0 \\ 0 & m_{b_2} \end{pmatrix},
\end{aligned} \tag{3.5}$$

where M^t, M^b represent the 2×2 mass mixing matrix between the t, T and b, B states, before diagonalization. The eigenvectors now become, for instance, for the top sector

$$\begin{aligned}
m^2_{t_1,t_2} = \frac{1}{4}&[(y_t^2 + y_T^2)v^2 + y_M^2 u^2] \\
&\times \left[1 \pm \sqrt{1 - \left(\frac{2 y_t y_M v u}{(y_t^2 + y_T^2)v^2 + y_M^2 u^2}\right)^2}\right]
\end{aligned} \tag{3.6}$$

with eigenvectors

$$\begin{pmatrix} t_1 \\ t_2 \end{pmatrix}_{L,R} = \begin{pmatrix} \cos\theta_{L,R} & \sin\theta_{L,R} \\ -\sin\theta_{L,R} & \cos\theta_{L,R} \end{pmatrix} \begin{pmatrix} t \\ T \end{pmatrix}_{L,R}, \tag{3.7}$$

where the mixing angles are

$$\begin{aligned}
\tan\theta_L &= \frac{2 y_T y_M v u}{y_M^2 u^2 - (y_t^2 + y_T^2)v^2} \\
\tan\theta_R &= \frac{2 y_t y_T v^2}{y_M^2 u^2 - (y_t^2 + y_T^2)v^2},
\end{aligned} \tag{3.8}$$

and similarly for the b-quark sector, with the replacement $t \to b$ and $\theta \to \beta$. Note that, because of their charge assignments, the X and Y fields do not mix with the other fermions and are therefore also mass eigenstates.

Relationships between mixing angles and mass eigenstates depend on the representation [43,44].

$$\begin{aligned}
\text{For doublets: } (XT):\ & m_X^2 = m_T^2(\cos\theta_R)^2 + m_t^2(\sin\theta_R)^2 \\
(TB):\ & m_T^2(\cos\theta_R)^2 + m_t^2(\sin\theta_R)^2 = m_B^2(\cos\beta_R)^2 + m_b^2(\sin\beta_R)^2 \\
(BY):\ & m_Y^2 = m_B^2(\cos\beta_R)^2 + m_b^2(\sin\beta_R)^2 \\
\\
\text{For triplets: } (XTB):\ & m_X^2 = m_T^2(\cos\theta_L)^2 + m_t^2(\sin\theta_L)^2 \\
& = m_B^2(\cos\beta_L)^2 + m_b^2(\sin\beta_L)^2, \\
\text{where } & \sin(2\beta_L) = \sqrt{2}\frac{m_T^2 - m_t^2}{(m_B^2 - m_b^2)}\sin(2\theta_L). \\
(TBY):\ & m_Y^2 = m_B^2(\cos\beta_L)^2 + m_b^2(\sin\beta_L)^2 \\
& = m_T^2(\cos\theta_L)^2 + m_t^2(\sin\theta_L)^2, \\
\text{where } & \sin(2\beta_L) = \frac{m_T^2 - m_t^2}{\sqrt{2}(m_B^2 - m_b^2)}\sin(2\theta_L),
\end{aligned} \tag{3.9}$$

and where

$$\begin{aligned}
m_T\tan\theta_R &= m_t\tan\theta_L \quad \text{for singlets, triplets} \\
m_T\tan\theta_L &= m_t\tan\theta_R \quad \text{for doublets} \\
m_B\tan\beta_R &= m_b\tan\beta_L \quad \text{for singlets, triplets} \\
m_B\tan\beta_L &= m_b\tan\beta_R \quad \text{for doublets.}
\end{aligned} \tag{3.10}$$

For doublet models, while the Higgs mixing is the same as in the previous section, the mixing between the top quark t and the new vectorlike singlet T, characterized by the mixing θ_L, results in the shift in the Yukawa couplings as follows

$$\begin{aligned}
y_t(\mu_0) &= \frac{\sqrt{2}m_t}{v}\frac{1}{\sqrt{\cos^2\theta_L + x_t^2\sin^2\theta_L}}, \\
y_T(\mu_0) &= \frac{\sqrt{2}m_T}{v}\frac{\sin\theta_L\cos\theta_L(1-x_t^2)}{\sqrt{\cos^2\theta_L + x_t^2\sin^2\theta_L}}, \\
y_B(\mu_0) &= \frac{\sqrt{2}m_B}{v}\frac{\sin\theta_L\cos\theta_L(1-x_b^2)}{\sqrt{\cos^2\theta_L + x_t^2\sin^2\theta_L}}, \\
y_M(\mu_0) &= \frac{m_T + m_B}{\sqrt{2}u}\sqrt{\cos^2\theta_L + x_t^2\sin^2\theta_L},
\end{aligned} \tag{3.11}$$

with $x_b = m_b/m_B$, and as before $x_t = m_t/m_T$. We use these expressions as initial conditions to the RGE equations, Eq. (A7). We review the mass bounds on vectorlike quarks, then proceed with our numerical analysis in Sec. III C.

B. Experimental bounds on vectorlike quark masses

Searches for vectorlike quarks have been performed at the LHC and various limits exist [45], all obtained assuming specific decay mechanisms. The Run 2 results from the LHC have improved previous limits from Run 1 by about 500 GeV [46]. All measurements assume top and down-type vectorlike quarks to decay into one of the final states involving Z, W or Higgs bosons with 100% branching ratios. So far, lower limits around 800 GeV have been obtained. The most recent search at ATLAS obtains, with 95% C.L., lower limits on the T mass of 870 GeV (890 GeV) for the singlet model, 1.05 TeV (1.06 TeV) for the doublet model, and 1.16 TeV (1.17 TeV) for the pure Zt decay mode quark [47]. The current experimental lower bound on the mass of the down-type vectorlike quark which mixes only with the third generation quark is around 730 GeV from Run 2 of the LHC and around 900 GeV from Run 1. The current lower bound for a vectorlike quark which mixes with the light quarks is around 760 GeV from Run 1. In our analyses, we set a lower limit on all masses of 800 GeV, to allow for the consideration of the largest parameter space. We proceed with analyzing the representations in turn, showing the effects of the additional fermions on the RGEs, and the mass and mixing angles constraints on the fermions and additional boson for each. All the relevant RGE for the Yukawa couplings, couplings between the bosons, and gauge coupling constants are given in the Appendix.

C. Numerical analysis

The evolution of the RGE's under different vectorlike fermion representations are illustrated in Fig. 8 for different values of the VEVs of the new scalar field ($u = 1$, 2, 4 TeV). In the case of $u = 1$ TeV, we have taken the mass of the scalar boson to be 0.8 TeV, because for $m_S = 1$ TeV, the Higgs sector couplings diverge, leading to singularities, whereas in the case of $u = 2$ TeV and $u = 4$ TeV, we chose $m_S = 1$ TeV because the smaller mass of 0.8 TeV is not large enough to ensure a positive Higgs quartic coupling. As required, all of the Higgs sector couplings remain positive up to Planck scale. As expected, the fermion Yukawa couplings tend to decrease with increasing

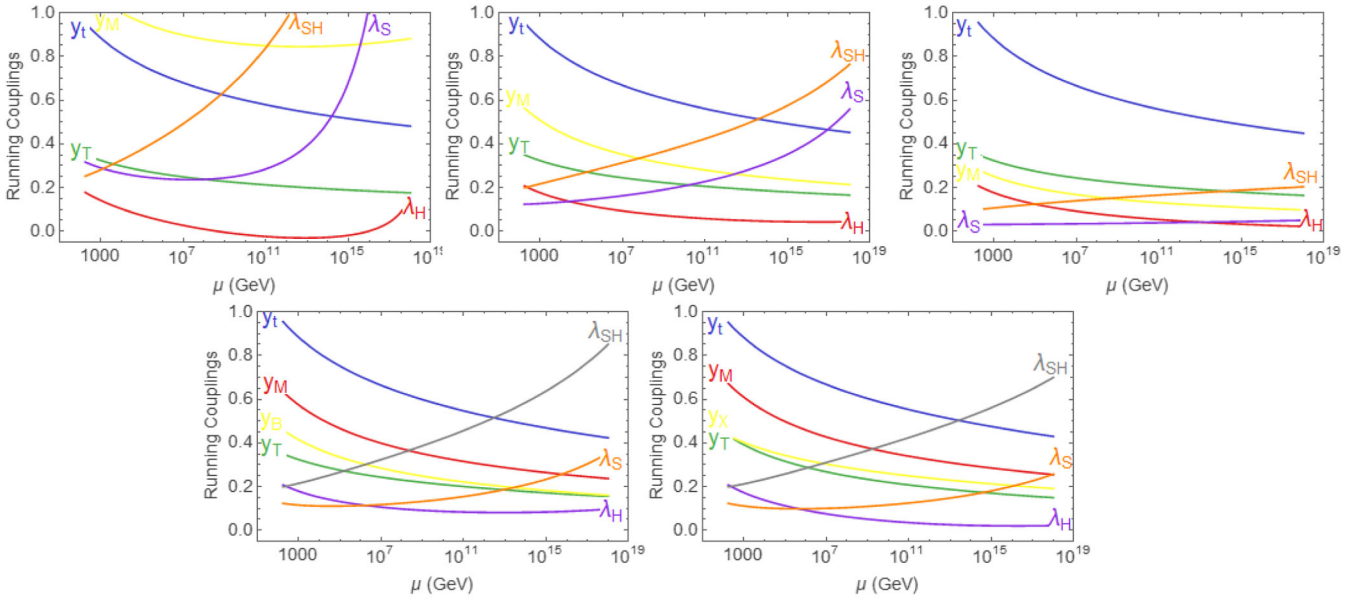

FIG. 8. The RGE running of the Yukawa and scalar couplings for models with vectorlike fermions. Top panel: singlet vectorlike representations, $\mathcal{D}_1$ and $\mathcal{U}_1$ fermion models. We have set $m_S = 0.8$ TeV, $u = 1$ TeV, (left panel), $m_S = 1$ TeV and $u = 2$ TeV (middle panel), and $m_S = 1$ TeV and $u = 4$ TeV (right panel). Bottom panel: the same for the doublet vectorlike models, for $u = 2$ TeV, (left panel) scalar + vectorlike (T, B), (right panel) scalar + vectorlike (X, T). For the doublet representations we took: $m_T = 0.8$ TeV, $m_B = 1$ TeV, $m_X = 1$ TeV, $m_S = 1$ TeV, $\mu_0 = m_t$, and mixing angles $\sin\varphi = 0.1$ and $\sin\theta_L = 0.08$.

energy, while the scalar bosonic couplings tend to increase. As we discussed previously, the addition of extra scalar bosons to the Standard Model helps maintain a positive Higgs self-coupling at larger energy scales, while the addition of extra fermions only aids in lowering it further. A common trend with respect to the models is that the Yukawa couplings are generally negatively affected by added loops at higher energy scales, while the Higgs sector couplings are generally affected positively (they tend to increase with increasing energy). The obvious exception here is the SM Higgs coupling, which strays dangerously close to zero at high energy scales, and even becomes negative for the additional singlet vectorlike fermion case. The models that augment the scalar boson by vectorlike representations vary significantly among each other in predictions for the various couplings with the scalar VEV u. Note in particular that for the first case, for the singlet vectorlike case, where $u = 1$, the Higgs couplings increase, and λ_H becomes negative at $\mu \sim 10^{11}$, rendering the theory unstable, while if the additional scalar VEV is increased to $u = 2$, or 4 TeV, the problem is ameliorated. The same problem recurs for the doublet and triplet models (not shown), but the theory is safe for $u = 2$ and 4 TeV. Differences in the running RGE's are more pronounced for λ_S, the new boson self-coupling, and negligible for the others. Note in particular, the difference between the values in Figs. 1 and 8. For the doublet and triplet vectorlike fermions, the RGE evolutions are similar, and the Higgs self-coupling remains positive at all energies. The additional scalar quartic coupling does not lie close to the origin as its interactions with fermions are small. There are some variations among models in the new scalar coupling, and the one describing the mixing with the SM Higgs. We have put less emphasis on the vacuum stability bound for the additional scalar, since its mass and VEV are unknown, and thus limiting concrete information from a detailed study of its vacuum stability bound.

Imposing the same conditions on the positivity of the potential as in Eq. (2.18), we study the allowed masses and mixing angles corresponding to each vectorlike fermion representation. In Figs. 9 and 10 we perform a scan over random values of the relevant vectorlike quarks between 300 and 2200 GeV, and for the mixing angles $\sin\beta_L$ (in the bottom sector) and $\sin\theta_L$ (in the top sector) between -1 and 1. The allowed values of the scalar mass m_S are plotted against the mixing angle in the scalar sector, $\sin\varphi$ for different values of the expectation values u (1, 2, and 4 TeV), providing an illustration of the possible quantitative properties of the scalar boson in this model. The results are given for all models. In Fig. 9 we plot the scans for singlet vectorlike T (top row), singlet vectorlike B (second row), (T, B) doublet (third row), (X, T) doublet (fourth row), (B, Y) doublet (bottom row). And in Fig. 10 we consider the (X, T, B) triplet (top row), and (T, B, Y) triplet (bottom row), providing an illustration of the possible quantitative properties of the scalar boson in these models. We remark from Figs. 9 and 10 that just as in the SM extension containing only an extra scalar boson, considered in the previous section, mass mixing between the two scalar bosons is always required, and this mixing is significant,

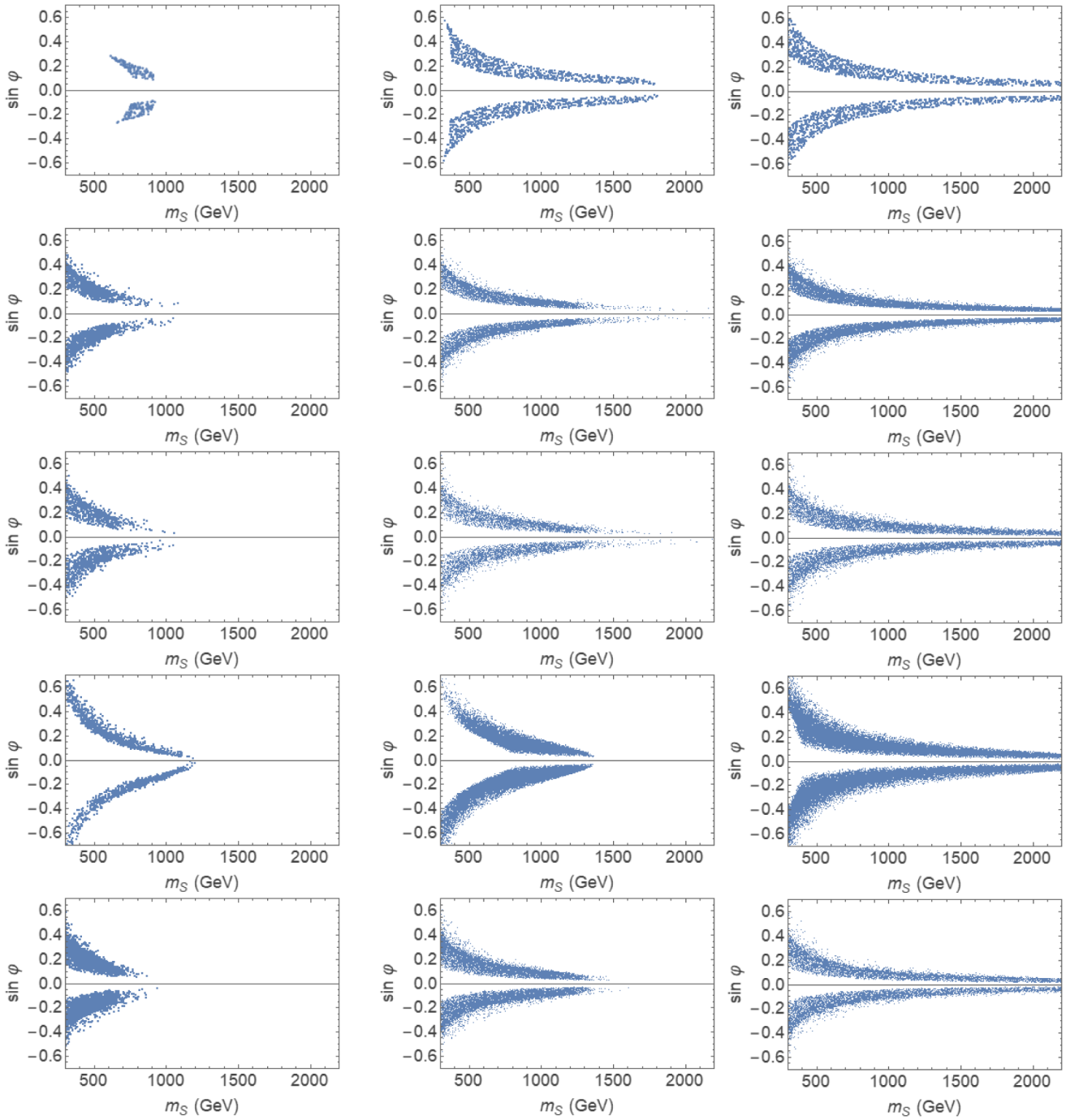

FIG. 9. The allowed parameter space for the scalar boson mass and mixing angle with the SM Higgs. In the (top panel) scalar + vectorlike T; (second panel) scalar + vectorlike B; (third panel) in the scalar + vectorlike (T, B) model; (fourth panel) scalar + vectorlike (X, T) fermion model; and (bottom panel) scalar + vectorlike (B, Y) fermion model, for different vacuum expectation values of the additional scalar: $u = 1$ TeV (left panel); $u = 2$ TeV (middle panel); and $u = 4$ TeV (right panel).

$\sin\varphi \geq 0.2$. Also, consistent with previous discussions, increasing the VEV u enlarges the parameter space, which is now quite restricted for $u = 1$ TeV. As expected, the addition of vectorlike fermions worsens the stability of the potential, but larger VEVs (mass scales) survive. The mixing in the singlet $\mathcal{U}_1$ model is the most effective counterterm addition, in fact pretty much ruling out the scenario where $u = 1$ TeV (unless the additional scalar is light, 600–1000 GeV), while the other representations provide much milder bounds for the same VEV.

We now investigate the restrictions on the vectorlike fermion masses and mixing from requiring the stability of the Higgs potential. We concentrate first on the vectorlike T, which has the same charge as the top quark, and which,

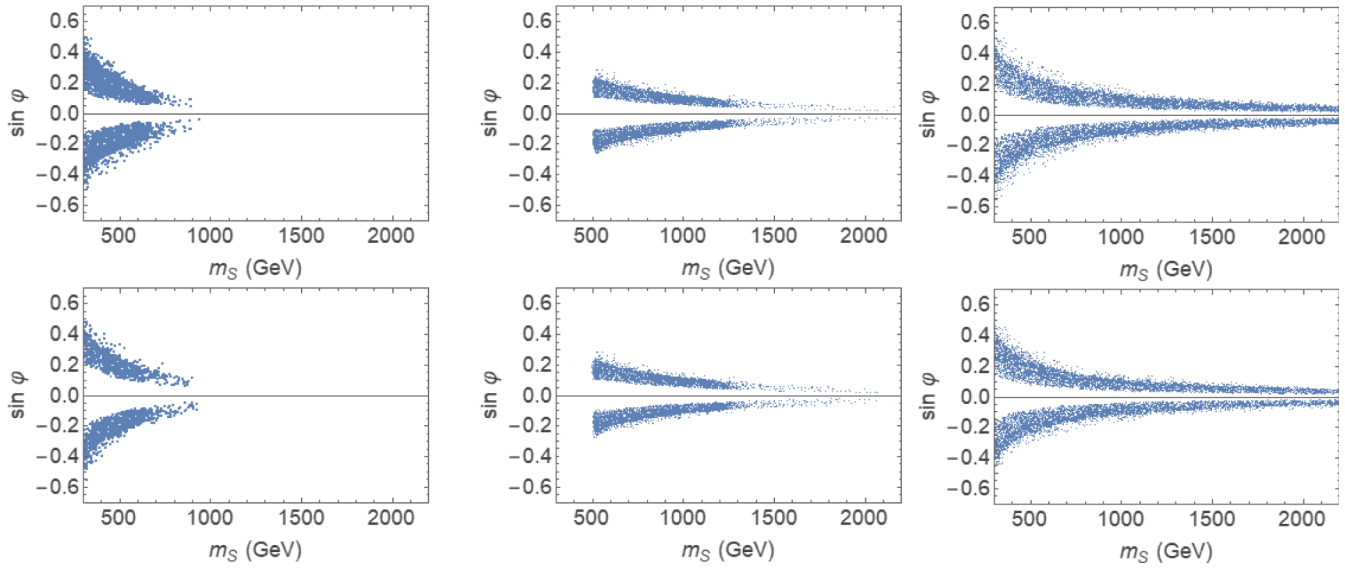

FIG. 10. (Continued) The allowed parameter space for the scalar boson mass and mixing angle with the SM Higgs. In the (top panel) the scalar + triplet (X,T,B) model, and for (bottom panel) the scalar + (T,B,Y) triplet model, for different vacuum expectation values of the additional scalar: $u=1$ TeV (left panel); $u=2$ TeV (middle panel); and $u=4$ TeV (right panel).

through mixing can affect changes in the Higgs potential, both in the fermion and in the scalar sector. In order to investigate this, we perform the same scan over random values of m_S and M_U between 300 and 2200 GeV, and for the mixing angles $\sin\varphi$ and $\sin\theta_L$ between -1 and 1, and show the results in Fig. 11. The first row shows the results for the singlet T vectorlike quark, the second row shows the results for the doublet vectorlike (T,B), the third for the (X,T) doublet, the fourth for the (X,T,B) triplet and the last for the (T,B,Y) triplet. Unlike the case of scalar mixing, here the mixing between the top quark and the vectorlike one is required to be small, in general, for most cases, in the region $\sin\theta_L \in (-0.2,0.2)$ (with some exceptions, where it can be larger, discussed below), and it can be zero. The allowed masses of the T quark are restricted for the scalar VEV $u=1$ TeV, and increase with increasing VEVs, so that in the singlet T and doublet (X,T) models cases, practically no T masses are allowed for $u=1$ TeV, while masses up to 1400 GeV are allowed for $u=4$ TeV. For the SM like doublet (T,B), for $u=1$ TeV, $m_T \leq 800$ GeV, for $u=2$ TeV, $m_T \leq 1600$ GeV, while for $u=4$ TeV, m_T spans the whole axis. Note that here, like in the scalar sector, there are marked differences between the scenarios. For the doublet (X,T), any mixing between the T and t quark is allowed. We expect this case to be somewhat similar to the singlet, however, the Yukawa coupling of the X quark lowers the Higgs coupling further, the parameter space continues to be severely constrained, and the mass is allowed in a narrow region near $m_T=1$ TeV for all values of the additional singlet. Here, as an exception to small mixing, the constraints on the mixing with the top are lifted. The case with triplets (X,T,B), affected by both the X and B vectorlike quarks, exhibits a behavior independent of the singlet VEV. Masses again are favored to be near $m_T=1$ TeV (we rule out light masses, ~500 from direct searches) and the mixing is allowed to be small or large. The strong enhancements are for the cases where the t and T mix. The mixing is expected to be stronger than between B and b quarks, due to the differences between mass of the top and of the bottom (making the denominator in Eq. (3.8) smaller). It is interesting to note here the effect of the X vectorlike quark, which, while not mixing with SM quarks, is nevertheless important for the mass of the T vectorlike quark [seen clearly if we compare the singlet T model with the doublet (X,T), and the doublet (T,B) model with the triplet (X,T,B)].

The scans in Fig. 12 illustrate the allowed masses and mixing angles of the B vectorlike quark with the bottom quark for the SM augmented by the additional scalar. We show, in the top panel, the vectorlike singlet B model, in the second panel, the vectorlike (T,B) model, in the third panel, the vectorlike (B,Y) model, in the fourth panel, in the vectorlike (X,T,B) triplet, and in the bottom panel, the (T,B,Y) triplet. We again perform the same scan over the m_B and m_S masses and mixing angles $\sin\beta_L$ constrained by vacuum stability requirement, and plot the resulting m_B against the mixing the b-sector $\sin\beta_L$. The effect of the B quark is markedly different from that of the T quark due to weaker constraints on its angle (the denominator in $\tan\beta_L$ is larger than $\tan\theta_L$). For the B singlet model, the mixing and mass range are restricted, especially for $u=1$ TeV, while for the (T,B) model the mass restrictions are lifted, but the mixing limits still remain. For the (B,Y) doublet and for the (T,B,Y) triplet model, the situation is very similar to that of the T mass and mixing in these models: the mixing is

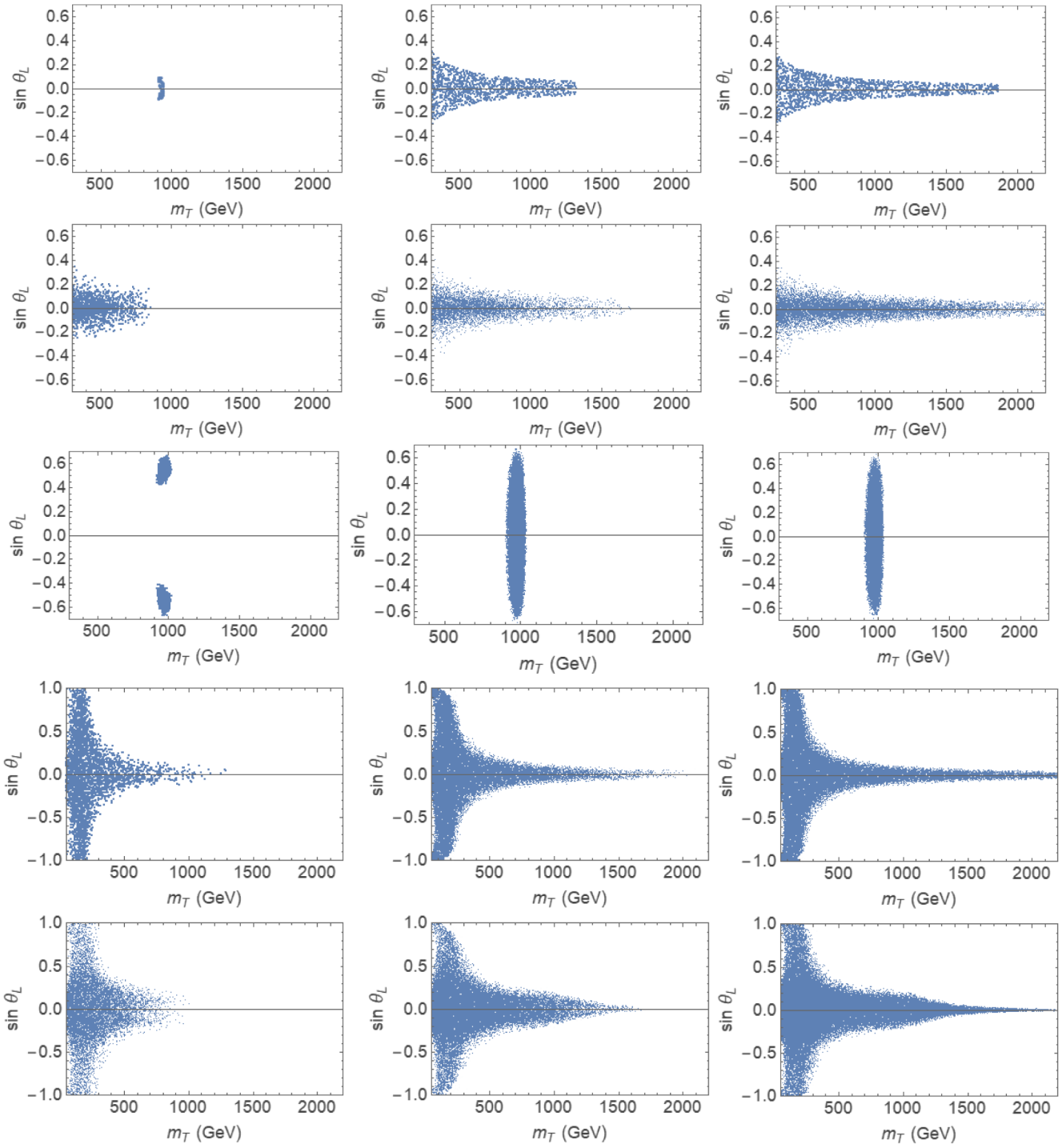

FIG. 11. The allowed parameter space for the T fermion mass and mixing angle with the top quark for: (top panel) in the scalar + singlet vectorlike T model; (second panel) in scalar + vectorlike (T, B) model; (third panel) for the T fermion mass and mixing angle in the scalar $+(X, T)$ fermion doublet model, (fourth panel) for the scalar $+(X, T, B)$ triplet, and (bottom panel) for the triplet (T, B, Y) model, for different vacuum expectation values, $u = 1$ TeV (left panel); $u = 2$ TeV (middle panel); and $u = 4$ TeV (right panel).

restricted everywhere except around 1000 GeV, and this result is independent on the scalar VEV.

Finally, we investigate constraints on the vectorlike fermions with non-SM like hypercharge, X, with charge $5/3$, and Y, with charge $-4/3$. As the additional vectorlike quarks X and Y do not mix with SM particle, a plot of mass against the mixing angle does not make sense, Instead, in Fig. 13, the allowed values of the scanned fermion mass m_X is plotted against m_T, and m_Y is correlated with m_B. Note that in the (X, T) quark doublet, the X and T masses are

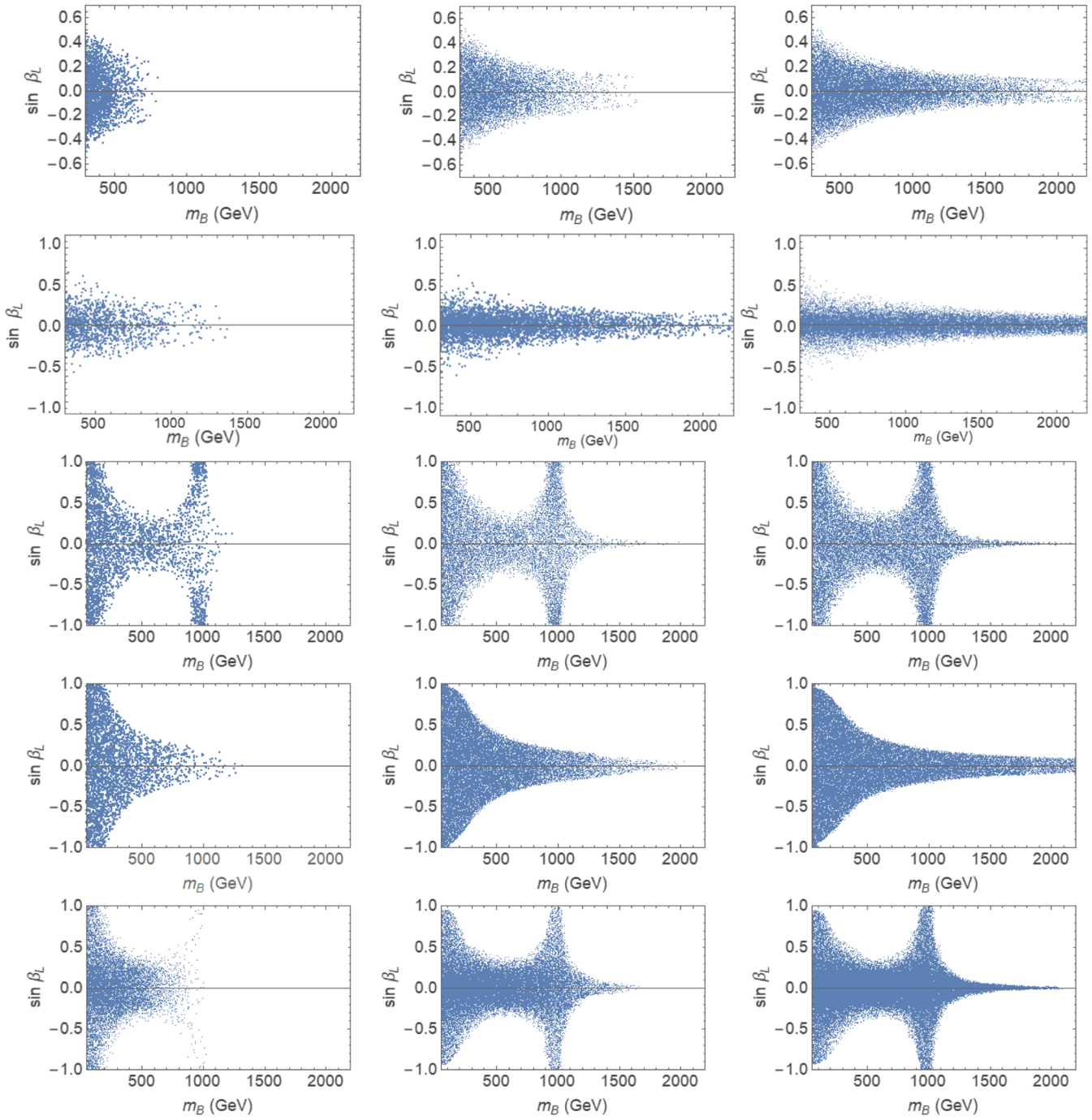

FIG. 12. The allowed parameter space for the B fermion mass and mixing angle in: (top panel) the vectorlike singlet B model, (second panel) the vectorlike (T, B) model, (third panel) the vectorlike (B, Y) model, (fourth panel) the vectorlike (X, T, B) triplet, and (bottom panel) the (T, B, Y) triplet, for different vacuum expectation values of the additional scalar: $u = 1$ TeV (left panel); $u = 2$ TeV (middle panel); and $u = 4$ TeV (right panel).

strongly correlated (as seen from the third row of Fig. 11) and the expected m_X is required to be close to 1000 GeV regardless of m_T values. We see that, similarly, in the (B, Y) doublet model, m_Y must have an allowed mass of approximately 1000 GeV, regardless of m_B, or the VEV u, unless both m_X and m_Y would be much lighter (100–200 GeV) in agreement with our earlier results. This seems to severely constrain models with vectorlike quarks with exotic hypercharges.

For completeness, all the relevant RGE for the Yukawa couplings, couplings between the bosons and coupling constants are included in the Appendix.

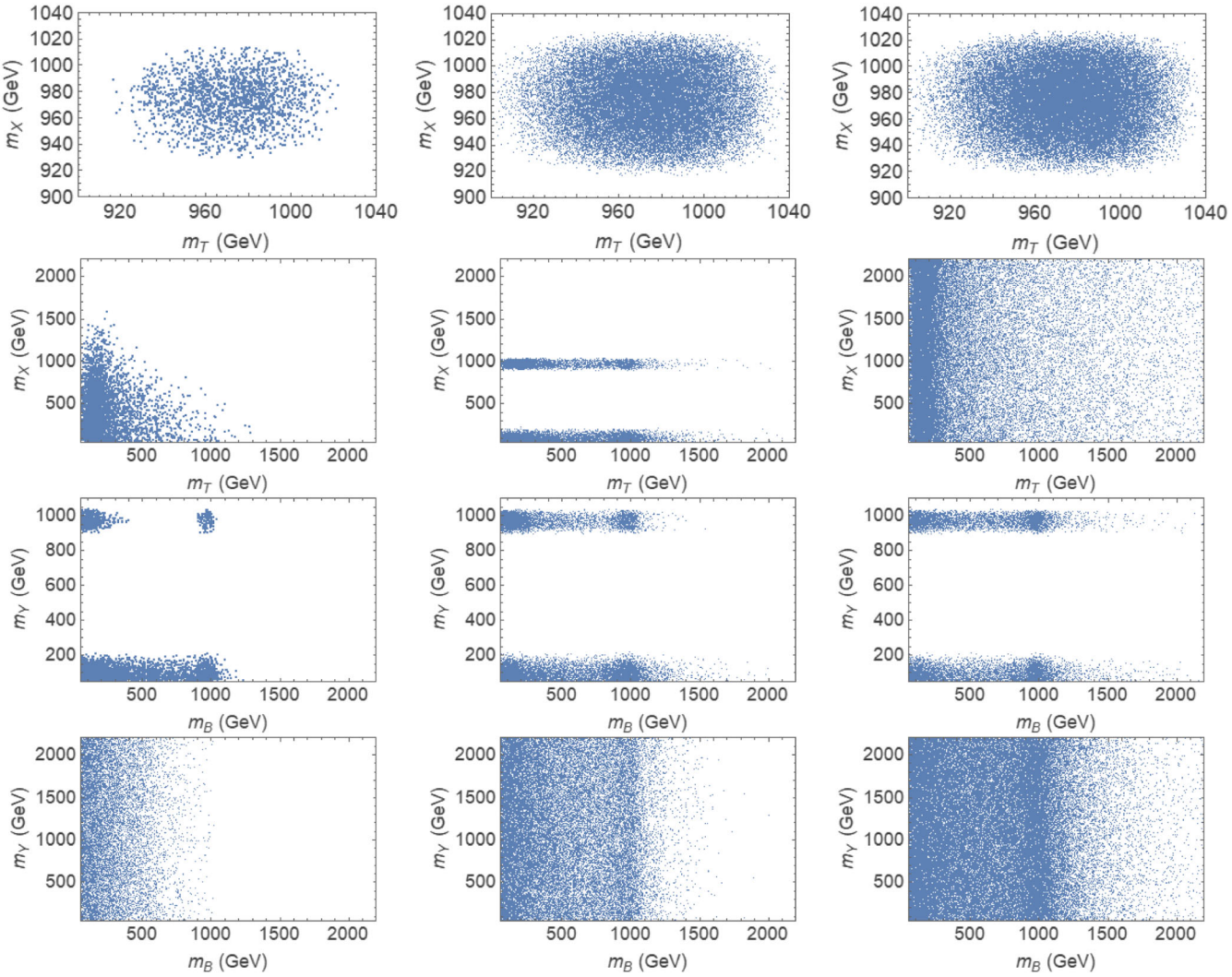

FIG. 13. The correlated parameter space for the X and T quark masses in the (X,T) quark doublet model (top panel) and in the (X,T,B) triplet model (second panel), and for the Y and B quark masses for the (B,Y) doublet model (third panel), and for the (T,B,Y) triplet model (bottom panel) for different vacuum expectation values.

IV. ELECTROWEAK PRECISION MEASUREMENTS

Constraints on possible new physics also emerge from precision electroweak measurements. The extra singlet scalar and vectorlike states induce modifications to the vacuum polarizations of electroweak gauge bosons at loop level, which are parametrized by the oblique parameters $\mathbb{S},\mathbb{T}$, and $\mathbb{U}$. For a large class of new physics models, corrections to precision electroweak observables are universal, in the sense that they are revealed only in self-energies of electroweak gauge bosons. There are solid constraints from these oblique corrections, pushing the scale of new physics around 1 TeV. The oblique parameters can be calculated perturbatively for any model from the gauge boson propagators, and are defined as [48].

$$\begin{aligned}\mathbb{S} &= 16\pi\Re[\bar{\Pi}_\gamma^{3Q}(m_Z^2) - \bar{\Pi}_Z^{33}(0)],\\ \mathbb{T} &= \frac{4\sqrt{2}G_F}{\alpha_e}\Re[\bar{\Pi}^{3Q}(0) - \bar{\Pi}^{11}(0)],\\ \mathbb{U} &= 16\pi\Re[\bar{\Pi}_Z^{33}(0) - \bar{\Pi}_W^{11}(0)]\end{aligned} \tag{4.1}$$

The current experimental values are obtained by fixing $\Delta\mathbb{U}=0$ are $\Delta\mathbb{T}=0.08\pm0.07$, $\Delta\mathbb{S}=0.05\pm0.09$. The overall calculation of $\mathbb{S},\mathbb{T}$, and $\mathbb{U}$ parameters via loop contributions can be separated into contributions from scalars and from fermions. Complete expressions for the contributions from the additional scalar and all fermion representations are given in the Appendix.

A. Contributions to the $\mathbb{S}$ and $\mathbb{T}$-parameters from scalar sector

Rewriting Eq. (4.1) explicitly in terms of the scalar loop contributions to the gauge boson two point functions

$$\begin{aligned}
\mathbb{S}_{SH} &= \frac{16\pi}{m_Z^2}\Re\left[\frac{c_w^2}{e g_z}(\Pi_{z\gamma}(m_Z^2)-\Pi_{z\gamma}(0)) + \frac{s_w^2 c_w^2}{e^2}(\Pi_{\gamma\gamma}(m_Z^2)-\Pi_{\gamma\gamma}(0)) + \frac{1}{g_z^2}(\Pi_{ZZ}(m_Z^2)-\Pi_{ZZ}(0))\right],\\
\mathbb{T}_{SH} &= \frac{1}{\alpha_e}\Re\left[-\frac{\Pi_{WW}(0)}{m_W^2} + \frac{\Pi_{ZZ}(0)}{m_Z^2} + \frac{2s_w}{c_w}\frac{\Pi_{\gamma Z}(0)}{m_Z^2} + \frac{s_w^2}{c_w^2}\frac{\Pi_{\gamma\gamma}(0)}{m_Z^2}\right],\\
\mathbb{U}_{SH} &= 16\pi\Re\left[\frac{1}{m_Z^2}\left(\frac{1}{g_z^2}(\Pi_{ZZ}(m_Z^2)-\Pi_{ZZ}(0)) + \frac{2s_w^2}{e g_z}(\Pi_{z\gamma}(m_Z^2)-\Pi_{Z\gamma}(0)) + \frac{s_w^4}{e^2}(\Pi_{\gamma\gamma}(m_Z^2)-\Pi_{\gamma\gamma}(0))\right)\right.\\
&\quad \left. + \frac{1}{g^2 m_W^2}(\Pi_{WW}(m_W^2)-\Pi_{WW}(0))\right]
\end{aligned} \tag{4.2}$$

Although pure scalar contributions to $\Delta\mathbb{S}$ and $\Delta\mathbb{T}$ relatively fit better with the experimental bounds as the scalar mixing angle is increased (Fig. 14), we are particularly interested in numerical values at $\sin\varphi \sim 0.1$ and $m_S \sim 1$ TeV since the constraints coming from vacuum stability are more restricted. Loop contributions from scalars to vector gauge boson two point functions are modified via scalar mixing and given in [49].

Moreover, in Fig. 14, it is seen that the whole scalar parameter space m_S, $\sin\varphi$ is allowed, considering only the constraints from oblique parameters.

B. VLQ contributions to the $\mathbb{S}$ and $\mathbb{T}$ parameters

The oblique correction parameter $\mathbb{T}$ for vectorlike quarks is given as [50]

$$\begin{aligned}
\mathbb{T} = \frac{N_c}{16\pi s_w^2 c_w^2}\left[\sum_{\alpha,i}[(|V_{\alpha i}^L|^2 + |V_{\alpha i}^R|^2)\theta_+(y_\alpha, y_i) + 2\mathrm{Re}(V_{\alpha i}^L V_{\alpha i}^{R*})\theta_-(y_\alpha, y_i)]\right.\\
- \sum_{\alpha,\beta}[(|U_{\alpha\beta}^L|^2 + |U_{\alpha\beta}^R|^2)\theta_+(y_\alpha, y_\beta) + 2\mathrm{Re}(U_{\alpha\beta}^L U_{\alpha\beta}^{R*})\theta_-(y_\alpha, y_\beta)]\\
\left. - \sum_{i,j}[(|D_{ij}^L|^2 + |D_{ij}^R|^2)\theta_+(y_i, y_j) + 2\mathrm{Re}(D_{ij}^L D_{ij}^{R*})\theta_-(y_i, y_j)]\right],
\end{aligned} \tag{4.3}$$

where the fermion ratio functions $\theta_\pm$ are given as

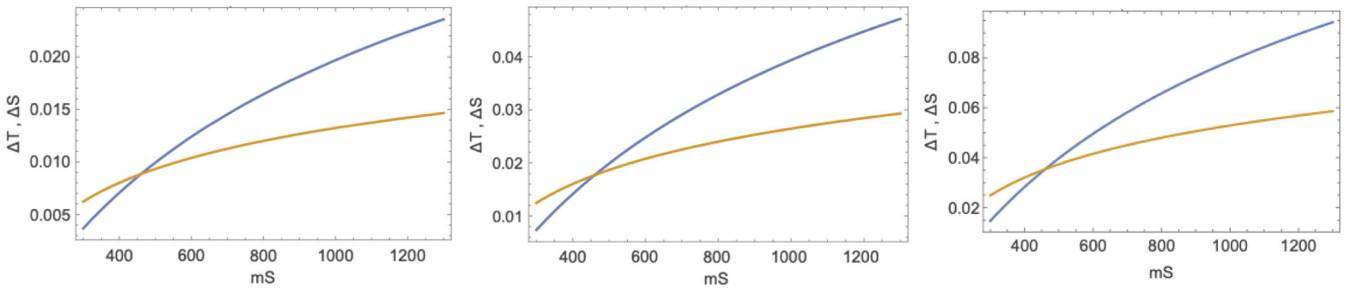

(a) $\sin\varphi = 0.1$ (b) $\sin\varphi = 0.2$ (c) $\sin\varphi = 0.4$

FIG. 14. The contribution to the $\mathbb{T}$ (orange) and $\mathbb{S}$ (blue) parameters in the SM augmented by a singlet scalar, as a function of the singlet scalar mass. We take $u = 1$ TeV for our consideration to remain in the vicinity of vacuum stability constraints.

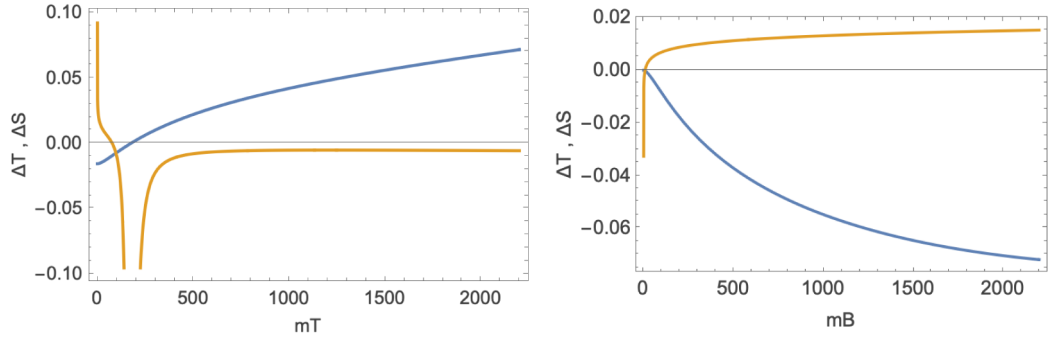

(a) $\mathcal{U}_1$ (T) (b) $\mathcal{D}_1$ (B)

FIG. 15. The contributions to the $\mathbb{T}$ (blue) and $\mathbb{S}$ (orange) parameters in the singlet representations, as functions of the vectorlike quark mass.

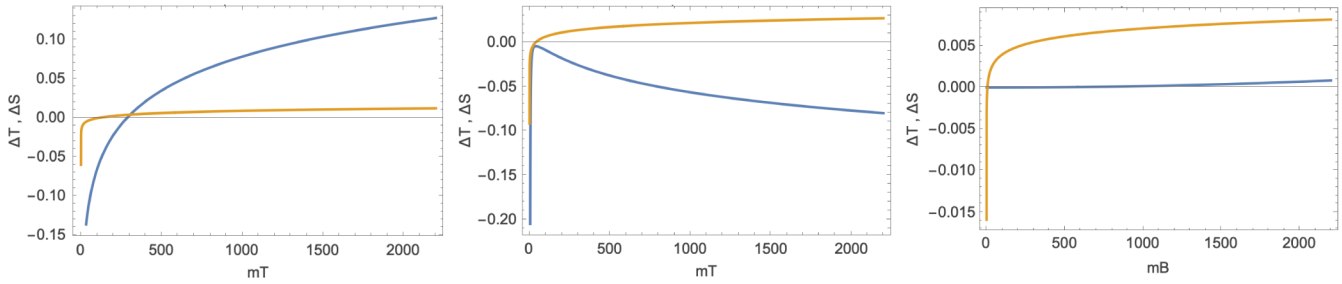

(a) $\mathcal{D}_2$ (T,B) (b) $\mathcal{D}_X$ (X,T) (c) $\mathcal{D}_Y$ (B,Y)

FIG. 16. The contributions to the $\mathbb{T}$ (blue) and $\mathbb{S}$ (orange) parameters in the doublet representations as functions of the vectorlike quark mass.

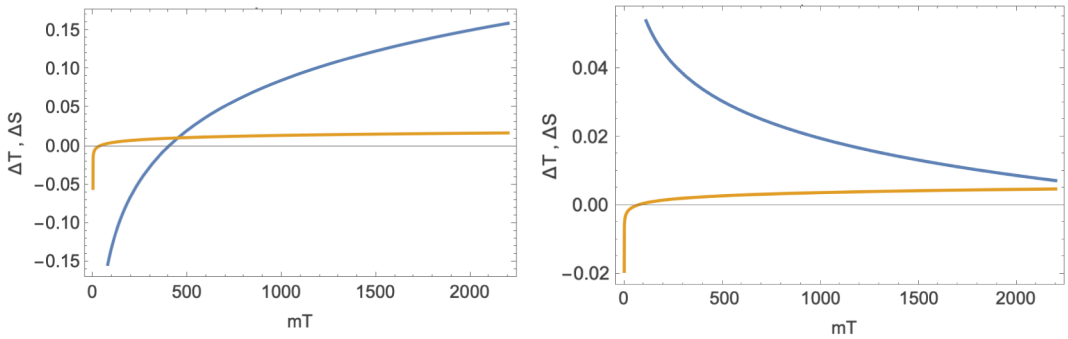

(a) $\mathcal{T}_X$ (X,T,B) (b) $\mathcal{T}_Y$ (T,B,Y)

FIG. 17. The contributions to the $\mathbb{T}$ (blue) and $\mathbb{S}$ (orange) parameters in the triplet representations, as functions of the vectorlike quark mass.

$$\theta_+ = y_1 + y_2 - \frac{2y_1y_2}{y_1 - y_2}\ln\frac{y_1}{y_2},$$
$$\theta_- = 2\sqrt{y_1y_2}\left(\frac{y_1 + y_2}{y_1 - y_2}\ln\frac{y_1}{y_2} - 2\right), \tag{4.4}$$

where $y_i = (\frac{m_i}{m_Z})^2$, and for the $\mathbb{S}$ parameter,

$$\mathbb{S} = \frac{N_c}{2\pi}\left[\sum_{\alpha,i}[(|V^L_{\alpha i}|^2 + |V^R_{\alpha i}|^2)\psi_+(y_\alpha, y_i) + 2\mathrm{Re}(V^L_{\alpha i}V^{R*}_{\alpha i})\psi_-(y_\alpha, y_i)]\right.$$
$$- \sum_{\alpha,\beta}[(|U^L_{\alpha\beta}|^2 + |U^R_{\alpha\beta}|^2)\chi_+(y_\alpha, y_\beta) + 2\mathrm{Re}(U^L_{\alpha\beta}U^{R*}_{\alpha\beta})\chi_-(y_\alpha, y_\beta)]$$
$$\left. - \sum_{i,j}[(|D^L_{ij}|^2 + |D^R_{ij}|^2)\chi_+(y_i, y_j) + 2\mathrm{Re}(D^L_{ij}D^{R*}_{ij})\chi_-(y_i, y_j)]\right], \tag{4.5}$$

where $V^{L,R}_{\alpha i}$, $U^{L,R}_{\alpha\beta}$, and $D^{L,R}_{ij}$ can be found in [43], and the functions $\psi_\pm$,$\chi_\pm$ are given respectively by

$$\psi_+ = \frac{22y_\alpha + 14y_i}{9} - \frac{1}{9}\ln\frac{y_\alpha}{y_i} + \frac{1 + 11y_\alpha}{18}f(y_\alpha, y_\alpha) + \frac{7y_i - 1}{18}f(y_i, y_i),$$
$$\psi_- = -\sqrt{y_\alpha y_i}\left(4 + \frac{f(y_\alpha, y_\alpha) + f(y_i, y_i)}{2}\right) \tag{4.6}$$

$$\chi_+ = \frac{y_1 + y_2}{2} - \frac{(y_1 - y_2)^2}{3} + \left[\frac{(y_1 - y_2)^3}{6} - \frac{1}{2}\frac{y_1^2 + y_2^2}{y_1 - y_2}\right]\ln\frac{y_1}{y_2} + \frac{y_1 - 1}{6}f(y_1, y_1)$$
$$+ \frac{y_2 - 1}{6}f(y_2, (y_2) + \left[\frac{1}{3} - \frac{y_1 + y_2}{6} - \frac{(y_1 - y_2)^2}{6}\right]f(y_1, y_2)$$
$$\chi_- = -\sqrt{y_1 y_2}\left[2 + \left(y_1 - y_2 - \frac{y_1 + y_2}{y_1 - y_2}\right)\ln\frac{y_1}{y_2} + \frac{f(y_1, y_1) + f(y_2, y_2)}{2} - f(y_1, y_2)\right]. \tag{4.7}$$

We now scan over different vectorlike fermion masses via approximate expressions with only leading order terms A 3.

We show the results for the oblique parameters for the vector-like quarks in the singlet representation in Fig. 15, in the doublet representation in Fig. 16, and in the triplet representation in Fig. 17. The $\mathbb{S}$-parameter agrees with the experimental bounds for small mixing angles, and does not bring tighter constraints on the masses of vectorlike quarks. However, the $\mathbb{T}$-parameter becomes negative for small mixing angles for the $\mathcal{D}_1$ and $\mathcal{D}_X$ representations. This feature in return might exclude some regions of the parameter space once combined with the contributions from the SM + additional scalar, and imposes further conditions on the mass of singlet scalar. Apart from the vacuum stability constraints that connects the two sectors, this unique feature of electroweak precision accounts for the destructive interference between parameter spaces of scalars and vectorlike fermions. Similar studies have been carried out in the literature [51] to impose more restricted constraints on parameter spaces of additional scalars. Checking the Eq. (A21) for $\Delta\mathbb{T}$, the logarithmic term suppress the linear term in the small mixing domain of $\mathcal{D}_1$. Similarly, for $\mathcal{D}_X$, the first term in Eq. (A23) is inversely proportional to vectorlike quark mass, which is rapidly suppressed by the second term, growing with opposite sign with respect to mass of vectorlike quark. Numerical values for $\Delta\mathbb{T}$ and $\Delta\mathbb{S}$ at $m_{VLQ} \sim 1$ TeV agree with the experimental limits in small mixing throughout all representations. However, it is shown from the mutual regions satisfying S, T-parameters and vacuum stability parameter spaces that, in general, vectorlike quark masses and mixings are inversely proportional to each other. Moreover, in the mixing interval $\sin\theta_{L,R} > 0.3$, although not shown here, $\Delta\mathbb{T}$ and $\Delta\mathbb{S}$ dangerously stray away from the experimental bounds, yielding more restrictions on m_S, as seen in Fig. 14. Therefore, negative contributions to $\Delta\mathbb{T}$ and $\Delta\mathbb{S}$ are very likely to be compensated with relatively heavier scalars in various models.

V. CONCLUSIONS

In this work, we presented a detailed analysis of the stability conditions on the Higgs potential under the presence of extra vectorlike fermions. Since these have the same couplings for left and right components, they do not affect the loop-induced decays of the SM Higgs boson, and indeed, can have arbitrary bare masses in the Lagrangian. We asked the question of whether they can have an effect on the Higgs sector, in particular, we concentrated on one of the outstanding problems in the SM, vacuum stability of the Higgs potential. While vectorlike fermions appear in many beyond the SM models, here we have taken a model-independent approach. We allowed mixing of the vectorlike fermions with the third generation chiral fermions only, and we considered all possible anomaly-free possibilities for the vectorlike representations, with the additional fermions allowed to be in singlet, doublet, or triplet representations.

As all other fermions, their effect on the RGE's of the Higgs self-coupling constant is to lower it further,

worsening the vacuum stability. An additional boson is introduced to alleviate this problem (representing an additional Higgs boson which would naturally appear in most new physics models). Its presence is essential, and by itself it remedies the stability problem. The allowed additional scalar mass varies with its assigned VEV, but for all scenarios the mixing with the SM Higgs is required to be nonzero. We analyze constraints on the parameter space coming from theory, experiment and cosmology, and accordingly, we require the singlet mass to be preferably in the $\mathcal{O}(\mathrm{TeV})$ scale. Thus this work focuses on TeV scale with small mixing because once vectorlike quarks are introduced, stability becomes the most restrictive theoretical constraint. Even in bare HSM (without vectorlike quarks), stability is one of the most stringent ones. In addition, the singlet scalar VEV must be in the TeV scale as well, as smaller VEVs spoil pertubativity and severely restrict the parameter space.

Additional fermionic representations survive for scalar VEVs $u = 1$, 2 or 4 TeV, and the agreement improves with increasing the scalar VEVs, indicating that higher scale physics is more likely to improve the vacuum stability problem. For most models, $u = 1$ TeV is highly restricted, and likely ruled out, especially for toplike vector fermions, or in doublet models where this fermion is the only one mixing with the SM top. The situation worsens for the (X, T) doublet model, where for all values of the VEV u, the mass m_T hovers around 1000 GeV and is independent of the mixing. For triplet representations, the parameter spaces for $T - t$ mixing have similar characteristics in imposing a small vectorlike quark mass limit, regardless of the value for the singlet VEV. Compared to the doublet (T, B) representation, large mixing angles are permitted, for a relatively wide allowed mass spectrum. Comparatively, the model (X, T, B) is more sensitive to large vectorlike quark masses, and shrinks the mixing angles to a small range as m_T becomes large, whereas the model (T, B, Y) allows for more parameter space for masses and mixing angles space for various singlet VEVs. The differences in parameter spaces can be attributed to the fact that although the vectorlike quark X does not mix with the SM particles, its Yukawa term appears in the RGE for y_T, which is unique to the (X, T, B) model.

Vacuum stability is improved if the bottomlike fermion is also present, and allowed to mix with the b quark. The mixing angles are in general small (an exception are extreme cases where the mass is extremely restricted and the mixing completely free). However the difference between models with toplike or bottomlike quarks offer a way to distinguish between them, complimentary to collider searches.

Compared to T vectorlike quarks, constraints on the B-like fermion masses and mixing angles are much more relaxed. For the (T, B) doublet model, the restrictions affect mostly m_T and are relaxed for m_B (the mixing with the b quark is required to be small). While the mixing can be larger for the (B, Y) and (T, B, Y) models, and for $m_B = 1000$ GeV, the mixing with the bottom quark is unrestricted. (On the other hand, the models (T, B, Y) and (B, Y) have almost identical parameter spaces for B mixings regardless of the singlet VEV. The mixings are constrained everywhere except $m_B = 1000$ GeV. Although its possible, the model (T, B, Y) is relatively less sufficient to impose mass values for m_B around 1000 GeV for $u = 1$ TeV. And finally, B mixings become less relaxed as the mass of vectorlike quark gets larger for the models (T, B) and (X, T, B).) The vectorlike quarks carrying non-SM hypercharge do not mix with quarks, and seem to be required to have masses of around 1000 GeV, irrespective of the model, other vectorlike fermion masses, or scalar VEV.

Compared to vacuum stability restrictions, electroweak precision constraints are more relaxed. Although the $\mathbb{S}$-parameter does not introduce strong restrictions on parameter space, the $\mathbb{T}$-parameter evolves in negative direction in different models. Combined with scalar contributions to $\mathbb{S}$ and $\mathbb{T}$-parameters, deviations from the experimental precision data might impose further restrictions on additional scalars and mixings with Higgs.

In conclusion, models where T-quark is unaccompanied by a B-quark yield very restrictive constraints for the masses m_T and mixing angles $\sin\theta_L$. As well, additional vectorlike fermions with hypercharge $5/3$ or $-4/3$ are shown to restricted the additional fermions to masses close to 1 TeV, for the sampled range of the parameter space, which, in association with their exotic charges, renders them predictable, making it easy to confirm or rule out the existence of these fermions. Our considerations which constrain the masses and mixings of vectorlike fermions are complimented by analyses on the parameters of models with vectorlike quarks from electroweak fits to the parameters in these models.

ACKNOWLEDGMENTS

We thank NSERC for partial financial support under Grant No. SAP105354.

APPENDIX

1. RGEs for SM + additional boson + vectorlike quarks

We give below the renormalization group equations for the models studied in the text. The original expressions appeared in [52], and more expressions are included in [18,22,23].

a. Singlet $\mathcal{U}_1(T)$, $Y = 2/3$

The relevant RGE for the Yukawa couplings are

$$\begin{aligned}
\frac{dy_t^2}{d\ln\mu^2} &= \frac{y_t^2}{16\pi^2}\left(\frac{9y_t^2}{2}+\frac{9y_T^2}{2}-\frac{17g_1^2}{20}-\frac{9g_2^2}{4}-8g_3^2\right),\\
\frac{dy_T^2}{d\ln\mu^2} &= \frac{y_T^2}{16\pi^2}\left(\frac{9y_t^2}{2}+\frac{9y_T^2}{2}+\frac{y_M^2}{4}-\frac{17g_1^2}{20}-\frac{9g_2^2}{4}-8g_3^2\right),\\
\frac{dy_M^2}{d\ln\mu^2} &= \frac{y_M^2}{16\pi^2}\left(y_T^2+\frac{9y_M^2}{2}-\frac{8g_1^2}{5}-8g_3^2\right).
\end{aligned} \tag{A1}$$

The Higgs sector RGEs, describing the interactions between the two bosons are

$$\begin{aligned}
\frac{d\lambda_H}{d\ln\mu^2} &= \frac{1}{16\pi^2}\left[\lambda_H\left(12\lambda_H+6y_t^2+6y_T^2-\frac{9g_1^2}{10}-\frac{9g_2^2}{2}\right)+\frac{\lambda_{SH}^2}{4}-3y_t^4-3y_T^4-6y_t^2y_T^2+\frac{27g_1^4}{100}+\frac{9g_2^4}{16}+\frac{9g_1^2g_2^2}{40}\right],\\
\frac{d\lambda_S}{d\ln\mu^2} &= \frac{1}{16\pi^2}(9\lambda_S^2+\lambda_{SH}^2+12y_M^2\lambda_S-12y_M^4),\\
\frac{d\lambda_{SH}}{d\ln\mu^2} &= \frac{1}{16\pi^2}\left[\lambda_{SH}\left(2\lambda_{SH}+6\lambda_H+3\lambda_S+3y_t^2+3y_T^2+6y_M^2-\frac{9g_1^2}{20}-\frac{9g_2^2}{4}\right)-12y_T^2y_M^2\right],
\end{aligned} \tag{A2}$$

b. Singlet $\mathcal{D}_1(B)$, $Y = -1/3$

The relevant RGE for the Yukawa couplings are

$$\begin{aligned}
\frac{dy_t^2}{d\ln\mu^2} &= \frac{y_t^2}{16\pi^2}\left(\frac{9y_t^2}{2}+\frac{3y_B^2}{2}-\frac{17g_1^2}{20}-\frac{9g_2^2}{4}-8g_3^2\right),\\
\frac{dy_B^2}{d\ln\mu^2} &= \frac{y_B^2}{16\pi^2}\left(\frac{3y_t^2}{2}+\frac{9y_B^2}{2}+\frac{y_M^2}{4}-\frac{g_1^2}{4}-\frac{9g_2^2}{4}-8g_3^2\right),\\
\frac{dy_M^2}{d\ln\mu^2} &= \frac{y_M^2}{16\pi^2}\left(y_B^2+\frac{9y_M^2}{2}-\frac{2g_1^2}{5}-8g_3^2\right).
\end{aligned} \tag{A3}$$

The Higgs sector RGEs, describing the interactions between the two bosons are

$$\begin{aligned}
\frac{d\lambda_H}{d\ln\mu^2} &= \frac{1}{16\pi^2}\left[\lambda_H\left(12\lambda_H+6y_t^2+6y_B^2-\frac{9g_1^2}{10}-\frac{9g_2^2}{2}\right)+\frac{\lambda_{SH}^2}{4}-3y_t^4-3y_B^4+\frac{27g_1^4}{100}+\frac{9g_2^4}{16}+\frac{9g_1^2g_2^2}{40}\right],\\
\frac{d\lambda_S}{d\ln\mu^2} &= \frac{1}{16\pi^2}(9\lambda_S^2+\lambda_{SH}^2+12y_M^2\lambda_S-12y_M^4),\\
\frac{d\lambda_{SH}}{d\ln\mu^2} &= \frac{1}{16\pi^2}\left[\lambda_{SH}\left(2\lambda_{SH}+6\lambda_H+3\lambda_S+3y_t^2+3y_B^2+6y_M^2-\frac{9g_1^2}{20}-\frac{9g_2^2}{4}\right)-12y_B^2y_M^2\right],
\end{aligned} \tag{A4}$$

Finally, the coupling constants gain additional terms due to the new fermion, for both models $\mathcal{U}_1$, $\mathcal{D}_1$ with singlet fermions as follows:

$$\begin{aligned}
\frac{dg_1^2}{d\ln\mu^2} &= \frac{g_1^4}{16\pi^2}\left(\frac{41}{10}+\frac{4}{15}\right),\\
\frac{dg_2^2}{d\ln\mu^2} &= \frac{g_2^4}{16\pi^2}\left(-\frac{19}{6}\right),\\
\frac{dg_3^2}{d\ln\mu^2} &= \frac{g_3^4}{16\pi^2}\left(-7+\frac{2}{3}\right).
\end{aligned} \tag{A5}$$

c. Doublet $\mathcal{D}_2$ (T, B), $Y = 1/6$

The relevant RGE for the Yukawa couplings are

$$\begin{aligned}
\frac{dy_t^2}{d\ln\mu^2} &= \frac{y_t^2}{16\pi^2}\left(\frac{9y_t^2}{2}+\frac{9y_T^2}{2}+\frac{3y_B^2}{2}+\frac{y_M^2}{2}-\frac{17g_1^2}{20}-\frac{9g_2^2}{4}-8g_3^2\right),\\
\frac{dy_T^2}{d\ln\mu^2} &= \frac{y_T^2}{16\pi^2}\left(\frac{9y_t^2}{2}+\frac{9y_T^2}{2}+\frac{3y_B^2}{2}+\frac{y_M^2}{2}-\frac{17g_1^2}{20}-\frac{9g_2^2}{4}-8g_3^2\right),\\
\frac{dy_B^2}{d\ln\mu^2} &= \frac{y_B^2}{16\pi^2}\left(\frac{9y_t^2}{2}+\frac{3y_T^2}{2}+\frac{9y_B^2}{2}+\frac{y_M^2}{2}-\frac{17g_1^2}{20}-\frac{9g_2^2}{4}-8g_3^2\right),\\
\frac{dy_M^2}{d\ln\mu^2} &= \frac{y_M^2}{16\pi^2}\left(y_T^2+y_B^2+\frac{11y_M^2}{2}-\frac{g_1^2}{40}-\frac{9g_2^2}{2}-8g_3^2\right).
\end{aligned} \tag{A6}$$

The Higgs sector RGEs, describing the interactions between the two bosons are

$$\begin{aligned}
\frac{d\lambda_H}{d\ln\mu^2} &= \frac{1}{16\pi^2}\left[\lambda_H\left(12\lambda_H+6y_t^2+6y_T^2+6y_B^2-\frac{9g_1^2}{10}-\frac{9g_2^2}{2}\right)+\frac{\lambda_{SH}^2}{4}-3y_t^4-3y_T^4-3y_B^2-6y_t^2y_T^2\right.\\
&\quad\left.-12y_B^2y_T^2+\frac{27g_1^4}{400}+\frac{9g_2^4}{16}+\frac{9g_1^2g_2^2}{40}\right],\\
\frac{d\lambda_S}{d\ln\mu^2} &= \frac{1}{16\pi^2}(9\lambda_S^2+\lambda_{SH}^2+12y_M^2\lambda_S-12y_M^4),\\
\frac{d\lambda_{SH}}{d\ln\mu^2} &= \frac{1}{16\pi^2}\left[\lambda_{SH}\left(2\lambda_{SH}+6\lambda_H+3\lambda_S+3y_t^2+3y_T^2+3y_B^2+6y_M^2-\frac{9g_1^2}{20}-\frac{9g_2^2}{4}\right)-12y_T^2y_M^2-12y_B^2y_M^2\right],
\end{aligned} \tag{A7}$$

d. Doublet $\mathcal{D}_X$ (X, T), $Y = 7/6$

The relevant RGE for the Yukawa couplings are

$$\begin{aligned}
\frac{dy_t^2}{d\ln\mu^2} &= \frac{y_t^2}{16\pi^2}\left(\frac{9y_t^2}{2}+\frac{9y_T^2}{2}+\frac{9y_X^2}{2}+\frac{y_M^2}{2}-\frac{17g_1^2}{20}-\frac{9g_2^2}{4}-8g_3^2\right),\\
\frac{dy_T^2}{d\ln\mu^2} &= \frac{y_T^2}{16\pi^2}\left(\frac{9y_t^2}{2}+\frac{9y_X^2}{2}+\frac{9y_T^2}{2}+\frac{y_M^2}{2}-\frac{17g_1^2}{20}-\frac{9g_2^2}{4}-8g_3^2\right),\\
\frac{dy_X^2}{d\ln\mu^2} &= \frac{y_X^2}{16\pi^2}\left(\frac{9y_t^2}{2}+\frac{9y_X^2}{2}+\frac{9y_T^2}{2}+\frac{y_M^2}{2}-\frac{17g_1^2}{20}-\frac{9g_2^2}{4}-8g_3^2\right),\\
\frac{dy_M^2}{d\ln\mu^2} &= \frac{y_M^2}{16\pi^2}\left(y_T^2+y_X^2+\frac{11y_M^2}{2}-\frac{49g_1^2}{40}-\frac{9g_2^2}{2}-8g_3^2\right).
\end{aligned} \tag{A8}$$

The Higgs sector RGEs, describing the interactions between the two bosons are

$$\begin{aligned}
\frac{d\lambda_H}{d\ln\mu^2} &= \frac{1}{16\pi^2}\left[\lambda_H\left(12\lambda_H+6y_t^2+6y_T^2+6y_X^2-\frac{9g_1^2}{10}-\frac{9g_2^2}{2}\right)+\frac{\lambda_{SH}^2}{4}-3y_t^4-3y_T^4-3y_X^2-6y_t^2y_T^2\right.\\
&\quad\left.-12y_X^2y_T^2+\frac{27g_1^4}{400}+\frac{9g_2^4}{16}+\frac{9g_1^2g_2^2}{40}\right],\\
\frac{d\lambda_S}{d\ln\mu^2} &= \frac{1}{16\pi^2}(9\lambda_S^2+\lambda_{SH}^2+12y_M^2\lambda_S-12y_M^4),\\
\frac{d\lambda_{SH}}{d\ln\mu^2} &= \frac{1}{16\pi^2}\left[\lambda_{SH}\left(2\lambda_{SH}+6\lambda_H+3\lambda_S+3y_t^2+3y_T^2+3y_X^2+3y_M^2-\frac{9g_1^2}{20}-\frac{9g_2^2}{4}\right)-6y_T^2y_M^2-6y_X^2y_M^2\right],
\end{aligned} \tag{A9}$$

e. Additional non SM-like quark doublet $\mathcal{D}_Y$ (B, Y), $Y = -5/6$

The relevant RGE for the Yukawa couplings are

$$\begin{aligned}
\frac{dy_t^2}{d\ln\mu^2} &= \frac{y_t^2}{16\pi^2}\left(\frac{9y_t^2}{2}+\frac{3y_B^2}{2}+\frac{9y_Y^2}{2}+\frac{y_M^2}{2}-\frac{17g_1^2}{20}-\frac{9g_2^2}{4}-8g_3^2\right),\\
\frac{dy_B^2}{d\ln\mu^2} &= \frac{y_T^2}{16\pi^2}\left(\frac{3y_t^2}{2}+\frac{9y_B^2}{2}+\frac{9y_Y^2}{2}+\frac{y_M^2}{2}-\frac{17g_1^2}{20}-\frac{9g_2^2}{4}-8g_3^2\right),\\
\frac{dy_Y^2}{d\ln\mu^2} &= \frac{y_Y^2}{16\pi^2}\left(\frac{9y_t^2}{2}+\frac{9y_Y^2}{2}+\frac{9y_B^2}{2}+\frac{y_M^2}{2}-2g_1^2-\frac{9g_2^2}{4}-8g_3^2\right),\\
\frac{dy_M^2}{d\ln\mu^2} &= \frac{y_M^2}{16\pi^2}\left(y_B^2+y_Y^2+\frac{9y_M^2}{2}-\frac{8g_1^2}{5}-8g_3^2\right).
\end{aligned} \tag{A10}$$

The Higgs sector RGEs, describing the interactions between the two bosons are

$$\begin{aligned}
\frac{d\lambda_H}{d\ln\mu^2} &= \frac{1}{16\pi^2}\left[\lambda_H\left(12\lambda_H+6y_t^2+6y_B^2+6y_Y^2-\frac{9g_1^2}{10}-\frac{9g_2^2}{2}\right)+\frac{\lambda_{SH}^2}{4}-3y_t^4-3y_B^4-3y_Y^2+\frac{27g_1^4}{400}+\frac{9g_2^4}{16}+\frac{9g_1^2g_2^2}{40}\right],\\
\frac{d\lambda_S}{d\ln\mu^2} &= \frac{1}{16\pi^2}(9\lambda_S^2+\lambda_{SH}^2+12y_M^2\lambda_S-12y_M^4),\\
\frac{d\lambda_{SH}}{d\ln\mu^2} &= \frac{1}{16\pi^2}\left[\lambda_{SH}\left(2\lambda_{SH}+6\lambda_H+3\lambda_S+3y_t^2+3y_B^2+3y_Y^2+6y_M^2-\frac{9g_1^2}{20}-\frac{9g_2^2}{4}\right)-12y_B^2y_M^2-12y_Y^2y_M^2\right],
\end{aligned} \tag{A11}$$

The coupling constants gain additional terms due to the new fermion in all doublet models as follows:

$$\begin{aligned}
\frac{dg_1^2}{d\ln\mu^2} &= \frac{g_1^4}{16\pi^2}\left(\frac{41}{10}+\frac{10}{3}\right),\\
\frac{dg_2^2}{d\ln\mu^2} &= \frac{g_2^4}{16\pi^2}\left(-\frac{19}{6}+\frac{13}{6}\right),\\
\frac{dg_3^2}{d\ln\mu^2} &= \frac{g_3^4}{16\pi^2}\left(-7+\frac{4}{3}\right).
\end{aligned} \tag{A12}$$

f. Triplet $\mathcal{T}_X$ (X, T, B), $Y = 2/3$

The relevant RGE for the Yukawa couplings are

$$\begin{aligned}
\frac{dy_t^2}{d\ln\mu^2} &= \frac{y_t^2}{16\pi^2}\left(\frac{9y_t^2}{2}+\frac{9y_T^2}{2}+\frac{9y_X^2}{2}+\frac{3y_B^2}{2}+\frac{y_M^2}{4}-\frac{17g_1^2}{20}-\frac{9g_2^2}{4}-8g_3^2\right),\\
\frac{dy_T^2}{d\ln\mu^2} &= \frac{y_T^2}{16\pi^2}\left(\frac{9y_t^2}{2}+\frac{9y_X^2}{2}+\frac{9y_T^2}{2}+\frac{3y_B^2}{2}+\frac{y_M^2}{4}-\frac{17g_1^2}{20}-\frac{9g_2^2}{4}-8g_3^2\right),\\
\frac{dy_X^2}{d\ln\mu^2} &= \frac{y_T^2}{16\pi^2}\left(\frac{9y_t^2}{2}+\frac{9y_X^2}{2}+\frac{9y_T^2}{2}+\frac{3y_B^2}{2}+\frac{y_M^2}{4}-\frac{41g_1^2}{20}-\frac{9g_2^2}{4}-8g_3^2\right),\\
\frac{dy_B^2}{d\ln\mu^2} &= \frac{y_B^2}{16\pi^2}\left(\frac{3y_t^2}{2}+\frac{9y_B^2}{2}+\frac{9y_X^2}{2}+\frac{9y_T^2}{2}+\frac{y_M^2}{4}-\frac{17g_1^2}{20}-\frac{9g_2^2}{4}-8g_3^2\right),\\
\frac{dy_M^2}{d\ln\mu^2} &= \frac{y_M^2}{16\pi^2}\left(y_T^2+y_X^2+y_B^2+\frac{27y_M^2}{2}-\frac{8g_1^2}{5}-\frac{9g_2^2}{4}-8g_3^2\right).
\end{aligned} \tag{A13}$$

The Higgs sector RGEs, describing the interactions between the two bosons are

$$\frac{d\lambda_H}{d\ln\mu^2} = \frac{1}{16\pi^2}\left[\lambda_H\left(12\lambda_H + 6y_t^2 + 6y_T^2 + 6y_X^2 - \frac{9g_1^2}{5} - 9g_2^2\right) + \frac{\lambda_{SH}^2}{4} - 3y_t^4 - 3y_T^4 - 3y_X^2 - 6y_t^2y_T^2 + \frac{27g_1^4}{200} + \frac{9g_2^4}{8} + \frac{18g_1^2g_2^2}{40}\right],$$
$$\frac{d\lambda_S}{d\ln\mu^2} = \frac{1}{16\pi^2}(9\lambda_S^2 + \lambda_{SH}^2 + 12y_M^2\lambda_S - 12y_M^4),$$
$$\frac{d\lambda_{SH}}{d\ln\mu^2} = \frac{1}{16\pi^2}\left[\lambda_{SH}\left(2\lambda_{SH} + 6\lambda_H + 3\lambda_S + 6y_t^2 + 6y_T^2 + 6y_X^2 + 6y_M^2 - \frac{9g_1^2}{10} - \frac{9g_2^2}{2}\right) - 6y_T^2y_M^2 - 6y_B^2y_M^2 - 6y_X^2y_M^2\right], \quad \text{(A14)}$$

g. Triplet $\mathcal{T}_Y$ $(T, B, Y), Y = -1/3$

The relevant RGE for the Yukawa couplings are

$$\frac{dy_t^2}{d\ln\mu^2} = \frac{y_t^2}{16\pi^2}\left(\frac{3y_B^2}{2} + \frac{9y_t^2}{2} + \frac{9y_T^2}{2} + \frac{9y_Y^2}{2} + \frac{y_M^2}{2} - \frac{17g_1^2}{20} - \frac{9g_2^2}{4} - 8g_3^2\right),$$
$$\frac{dy_T^2}{d\ln\mu^2} = \frac{y_T^2}{16\pi^2}\left(\frac{3y_B^2}{2} + \frac{9y_t^2}{2} + \frac{9y_Y^2}{2} + \frac{9y_T^2}{2} + \frac{y_M^2}{2} - \frac{17g_1^2}{20} - \frac{9g_2^2}{4} - 8g_3^2\right),$$
$$\frac{dy_B^2}{d\ln\mu^2} = \frac{y_B^2}{16\pi^2}\left(\frac{3y_t^2}{2} + \frac{3y_T^2}{2} + \frac{9y_B^2}{2} + \frac{9y_Y^2}{2} + \frac{y_M^2}{4} - \frac{17g_1^2}{20} - \frac{9g_2^2}{4} - 8g_3^2\right),$$
$$\frac{dy_Y^2}{d\ln\mu^2} = \frac{y_Y^2}{16\pi^2}\left(\frac{3y_t^2}{2} + \frac{9y_B^2}{2} + \frac{9y_Y^2}{2} + \frac{9y_T^2}{2} + \frac{y_M^2}{2} - \frac{17g_1^2}{20} - \frac{9g_2^2}{4} - 8g_3^2\right),$$
$$\frac{dy_M^2}{d\ln\mu^2} = \frac{y_M^2}{16\pi^2}\left(y_T^2 + y_B^2 + y_Y^2 + \frac{15y_M^2}{2} - \frac{2g_1^2}{5} - 8g_3^2\right). \quad \text{(A15)}$$

The Higgs sector RGEs, describing the interactions between the two bosons are:

$$\frac{d\lambda_H}{d\ln\mu^2} = \frac{1}{16\pi^2}\left[\lambda_H\left(12\lambda_H + 6y_t^2 + 6y_B^2 + 6y_T^2 + 6y_Y^2 - \frac{9g_1^2}{5} - \frac{9g_2^2}{2}\right) + \frac{\lambda_{SH}^2}{4} - 6y_t^4 - 6y_T^4 - 6y_Y^4 - 3y_B^2 - 6y_t^2y_T^2 + \frac{27g_1^4}{200} + \frac{9g_2^4}{8} + \frac{18g_1^2g_2^2}{40}\right],$$
$$\frac{d\lambda_S}{d\ln\mu^2} = \frac{1}{16\pi^2}(9\lambda_S^2 + \lambda_{SH}^2 + 12y_M^2\lambda_S - 12y_M^4),$$
$$\frac{d\lambda_{SH}}{d\ln\mu^2} = \frac{1}{16\pi^2}\left[\lambda_{SH}\left(2\lambda_{SH} + 6\lambda_H + 3\lambda_S + 6y_t^2 + 6y_T^2 + 6y_B^2 + 6y_Y^2 + 6y_M^2 - \frac{9g_1^2}{10} - \frac{9g_2^2}{2}\right) - 6y_T^2y_M^2 - 6y_Y^2y_M^2 - 6y_B^2y_M^2\right], \quad \text{(A16)}$$

The coupling constants gain additional terms due to the new fermions in both triplet models as follows:

$$\frac{dg_1^2}{d\ln\mu^2} = \frac{g_1^4}{16\pi^2}\left(\frac{41}{10} + \frac{16}{5}\right),$$
$$\frac{dg_2^2}{d\ln\mu^2} = \frac{g_2^4}{16\pi^2}\left(-\frac{19}{6} + 4\right),$$
$$\frac{dg_3^2}{d\ln\mu^2} = \frac{g_3^4}{16\pi^2}(-7 + 2). \quad \text{(A17)}$$

2. Oblique parameters $\mathbb{S}$ and $\mathbb{T}$ in the scalar sector

We give below the conventional shifts in oblique parameters $\mathbb{S}$ and $\mathbb{T}$ from the SM. The original expressions appeared in [18] with only one singlet representation. Additional contributions to two point functions are also included in [49] for further analysis.

The explicit expressions for the $\Delta\mathbb{S}$ and $\Delta\mathbb{T}$ parameters for the SHM, including the extra singlet scalar representation, but without the vectorlike quarks, are

$$\Delta\mathbb{T} = \mathbb{T}_{SH} - \mathbb{T}_{\rm SM} = -\frac{3s_\phi^2}{16\pi c_w^2}([t_S] - [t_H]), \tag{A18}$$

where

$$[t_S] = ((m_S^2 - m_Z^2)(m_S^2 - m_W^2))^{-1}\left[m_S^4 \ln(m_S^2) - \frac{(m_S^2 - m_W^2)m_Z^2 \ln(m_Z^2) - m_W^2 \ln(m_W^2)c_w^2(m_S^2 - m_Z^2)}{s_w^2}\right]$$

and similarly for $[t_H]$ function, with the replacement $m_S \to m_H$.

$$\Delta\mathbb{S} = \mathbb{S}_{SH} - \mathbb{S}_{\rm SM} = \frac{s_\phi^2}{12\pi}\left(2\ln\left(\frac{m_S}{m_H}\right) + [s_S] - [s_H]\right) \tag{A19}$$

where

$$[s_S] = \frac{m_Z^4(9m_S^2 + m_Z^2)}{(m_S^2 - m_Z^2)^3}\ln\left(\frac{m_S^2}{m_Z^2}\right) - \frac{m_Z^2(4m_S^2 + 6m_Z^2)}{(m_S^2 - m_Z^2)^2}$$

and similarly for $[s_H]$ function, with the replacement $m_S \to m_H$.

3. Vectorlike quark contributions to the $\mathbb{S}$ and $\mathbb{T}$ parameters

a. Singlet $\mathcal{U}_1(T)$, $Y = 2/3$

$$\begin{aligned}\Delta\mathbb{T} &= \frac{m_t^2 N_c (s_L^t)^2}{16\pi c_w^2 s_w^2 m_Z^2}\left[x_T^2 (s_L^t)^2 - (c_L^t)^2 - 1 + 4(c_L^t)^2 \frac{m_T^2}{m_T^2 - m_t^2}\ln(x_T)\right],\\ \Delta\mathbb{S} &= \frac{N_c (s_L^t)^2}{18\pi}\left(\frac{(c_L^t)^2}{(x_T - 1)^3}[2\ln(x_T)(3 - 9x_T^2 - 9x_T^4 + 3x_T^6) + 5 - 27x_T^2 - 27x_T^4 - 5x_T^6] - 2\ln(x_T)\right)\end{aligned} \tag{A20}$$

b. Singlet $\mathcal{D}_1(B)$, $Y = -1/3$

$$\begin{aligned}\Delta\mathbb{T} &= \frac{m_t^2 N_c x_B}{16\pi c_w^2 s_w^2 m_Z^2 (x_B - 1)}[(s_L^b)^4 (x_B - 1) - 2(s_L^b)^2 \ln(x_B)],\\ \Delta\mathbb{S} &= \frac{N_c (s_L^b)^2}{18\pi}\left[2\ln\left(\frac{m_b}{m_B}\right)(3(s_L^b)^2 - 4) - 5(c_L^b)^2\right]\end{aligned} \tag{A21}$$

c. Doublet $\mathcal{D}_2$ (T,B), $Y = 1/6$

$$\Delta\mathbb{T} \simeq \frac{m_t^2 N_c (s_R^t)^2}{8\pi c_w^2 s_w^2 m_Z^2}[2\ln(x_T) - 2],$$
$$\Delta\mathbb{S} \simeq \frac{N_c}{18\pi}[(s_R^b)^2(2\ln(x_T) - 2\ln(x_b) - 2) + (s_R^t)^2(4\ln(x_T) - 7)] \tag{A22}$$

d. Doublet $\mathcal{D}_X$ (X,T), $Y = 7/6$

$$\Delta\mathbb{T} \simeq \frac{m_t^2 N_c (s_R^t)^2}{8\pi c_w^2 s_w^2 m_Z^2 (x_T - 1)}\left[\ln\left((c_R^t)^2 + \frac{(s_R^t)^2}{x_T}\right) - \ln(x_T)[x_T + \mathcal{O}(x_T^{-4})]\right],$$
$$\Delta\mathbb{S} \simeq \frac{N_c (s_R^t)^2}{18\pi}\left[3 + \ln(x_T) + \mathcal{O}\left(\frac{(s_R^t)^4}{x_B}\right)\right] \tag{A23}$$

e. Doublet $\mathcal{D}_Y$ (B,Y), $Y = -5/6$

$$\Delta\mathbb{T} \simeq \frac{m_t^2 N_c x_B}{128\pi c_w^2 s_w^2 m_Z^2}[-16c_R^b(-3 + c_R^{2b}\cot_R^b\ln(c_R^b)) + s_R^b(-13 - 20c_R^{2b} + 4c_R^{2b})],$$
$$\Delta S \simeq \frac{N_c}{144\pi}[-3\ln(x_B) + 20\ln(c_R^b) + \ln(x_b) + 19 + c_R^{4b}(5 + 3\ln(x_b)) + 4c_R^{2b}(-6 - \ln(x_b))] \tag{A24}$$

f. Triplet $\mathcal{T}_X$ (X,T,B), $Y = 2/3$

$$\Delta\mathbb{T} \simeq \frac{m_t^2 N_c (s_L^t)^2}{16\pi c_w^2 s_w^2 m_Z^2}[6\ln(x_T) - 10 + \mathcal{O}((s_L^t)^4, (c_L^t)^4, x_T^{-4})],$$
$$\Delta S \simeq -\frac{N_c (s_L^t)^2}{18\pi}[9 - 6\ln(x_T) + 4\ln(x_b) + \mathcal{O}((c_L^t)^4, (c_L^t)^2(s_L^t)^2)] \tag{A25}$$

g. Triplet $\mathcal{T}_Y$ (T,B,Y), $Y = -1/3$

$$\Delta\mathbb{T} \simeq -\frac{m_t^2 N_c (s_L^t)^2}{16\pi c_w^2 s_w^2 m_Z^2}[2\ln(x_T) - 6 + \mathcal{O}((s_L^t)^4, (c_L^t)^2(s_L^t)^2, x_T^{-3})],$$
$$\Delta\mathbb{S} \simeq \frac{N_c (s_L^t)^2}{18\pi}[2\ln(x_T) + 4 + \mathcal{O}((c_L^t)^4, (s_L^t)^4, (c_L^t)^2(s_L^t)^2)], \tag{A26}$$

where $x_i = \frac{m_F}{m_t}$ for all representations.

[1] G. Aad *et al.* (ATLAS Collaboration), Phys. Lett. B **716**, 1 (2012); S. Chatrchyan *et al.* (CMS Collaboration), Phys. Lett. B **716**, 30 (2012).

[2] G. Degrassi, S. Di Vita, J. Elias-Miró, J. R. Espinosa, G. F. Giudice, G. Isidori, and A. Strumia, J. High Energy Phys. 08 (2012) 098; D. Buttazzo, G. Degrassi, P. Paolo Giardino, G. F. Giudice, F. Sala, A. Salvio, and A. Strumia, J. High Energy Phys. 12 (2013) 089.

[3] F. Bezrukov, A. Magnin, M. Shaposhnikov, and S. Sibiryakov, J. High Energy Phys. 01 (2011) 016.

[4] F. Bezrukov, D. Gorbunov, and M. Shaposhnikov, J. Cosmol. Astropart. Phys. 06 (2009) 029.

[5] A. De Simone, M. P. Hertzberg, and F. Wilczek, Phys. Lett. B **678**, 1 (2009).
[6] C. P. Burgess, H. M. Lee, and M. Trott, J. High Energy Phys. 07 (2010) 007.
[7] M. Atkins and X. Calmet, Phys. Lett. B **697**, 37 (2011).
[8] I. Masina and A. Notari, Phys. Rev. D **85**, 123506 (2012); G. Isidori, V. S. Rychkov, A. Strumia, and N. Tetradis, Phys. Rev. D **77**, 025034 (2008); F. L. Bezrukov and M. Shaposhnikov, Phys. Lett. B **659**, 703 (2008); K. Kamada, T. Kobayashi, T. Takahashi, M. Yamaguchi, and J. Yokoyama, Phys. Rev. D **86**, 023504 (2012).
[9] J. F. Gunion and H. E. Haber, Phys. Rev. D **67**, 075019 (2003).
[10] J. A. Aguilar-Saavedra, Phys. Rev. D **67**, 035003 (2003); **69**, 099901(E) (2004).
[11] S. A. R. Ellis, R. M. Godbole, S. Gopalakrishna, and J. D. Wells, J. High Energy Phys. 09 (2014) 130; S. Dawson and E. Furlan, Phys. Rev. D **86**, 015021 (2012); J. A. Aguilar-Saavedra, R. Benbrik, S. Heinemeyer, and M. Perez-Victoria, Phys. Rev. D **88**, 094010 (2013); G. Cacciapaglia, A. Deandrea, D. Harada, and Y. Okada, J. High Energy Phys. 11 (2010) 159.
[12] S. Gopalakrishna, T. Mandal, S. Mitra, and G. Moreau, J. High Energy Phys. 08 (2014) 079.
[13] R. Contino, L. Da Rold, and A. Pomarol, Phys. Rev. D **75**, 055014 (2007); B. A. Dobrescu and C. T. Hill, Phys. Rev. Lett. **81**, 2634 (1998).
[14] C. Anastasiou, E. Furlan, and J. Santiago, Phys. Rev. D **79**, 075003 (2009).
[15] N. Arkani-Hamed, A. G. Cohen, E. Katz, and A. E. Nelson, J. High Energy Phys. 07 (2002) 034; Jay Hubisz and Patrick Meade, Phys. Rev. D **71**, 035016 (2005).
[16] S. P. Martin, Phys. Rev. D **81**, 035004 (2010); **82**, 055019 (2010).
[17] G. Couture, M. Frank, C. Hamzaoui, and M. Toharia, Phys. Rev. D **95**, 095038 (2017); A. Angelescu, A. Djouadi, and G. Moreau, Eur. Phys. J. C **76**, 99 (2016).
[18] M. L. Xiao and J. H. Yu, Phys. Rev. D **90**, 014007 (2014); **90**, 019901(A) (2014).
[19] G. Hiller, T. Höhne, D. F. Litim, and T. Steudtner, Phys. Rev. D **106**, 115004 (2022).
[20] D. Egana-Ugrinovic, J. High Energy Phys. 12 (2017) 064.
[21] S. P. He, arXiv:2205.02088.
[22] M. Dhuria and G. Goswami, Phys. Rev. D **94**, 055009 (2016).
[23] J. Zhang and S. Zhou, Chin. Phys. C **40**, 081001 (2016).
[24] D. Carmi, A. Falkowski, E. Kuflik, and T. Volansky, J. High Energy Phys. 07 (2012) 136; S. Dawson and E. Furlan, Phys. Rev. D **86**, 015021 (2012); J. Kang, P. Langacker, and B. D. Nelson, Phys. Rev. D **77**, 035003 (2008); S. Fajfer, A. Greljo, J. F. Kamenik, and I. Mustac, J. High Energy Phys. 07 (2013) 155.
[25] G. Altarelli and G. Isidori, Phys. Lett. B **337**, 141 (1994).
[26] Y. Tang, Mod. Phys. Lett. A **28**, 1330002 (2013).
[27] A. Sirlin and R. Zucchini, Nucl. Phys. **B266**, 389 (1986).
[28] P. Ghorbani, Nucl. Phys. **B971**, 115533 (2021).
[29] R. Hempfling and B. A. Kniehl, Phys. Rev. D **51**, 1386 (1995).
[30] A. Ilnicka, T. Robens, and T. Stefaniak, Mod. Phys. Lett. A **33**, 1830007 (2018).
[31] O. Lebedev, Prog. Part. Nucl. Phys. **120**, 103881 (2021).
[32] D. López-Val and T. Robens, Phys. Rev. D **90**, 114018 (2014).
[33] R. L. Workman *et al.* (Particle Data Group), Prog. Theor. Exp. Phys. **2022**, 083C01 (2022).
[34] M. E. Peskin and T. Takeuchi, Phys. Rev. D **46**, 381 (1992).
[35] M. Gorbahn, J. M. No, and V. Sanz, J. High Energy Phys. 10 (2015) 036.
[36] S. Kanemura, M. Kikuchi, K. Mawatari, K. Sakurai, and K. Yagyu, Nucl. Phys. **B949**, 114791 (2019).
[37] D. de Florian *et al.* (LHC Higgs Cross Section Working Group), arXiv:1610.07922.
[38] C. Sturm, B. Summ, and S. Uccirati, arXiv:2212.11835.
[39] Y. Xiao, J. M. Yang, and Y. Zhang, J. High Energy Phys. 02 (2023) 008.
[40] E. Fernández-Martínez, J. López-Pavón, J. M. No, T. Ota, and S. Rosauro-Alcaraz, arXiv:2210.16279.
[41] P. Athron, J. M. Cornell, F. Kahlhoefer, J. Mckay, P. Scott, and S. Wild, Eur. Phys. J. C **78**, 830 (2018).
[42] C. Balázs, Y. Xiao, J. M. Yang, and Y. Zhang, arXiv:2301.09283.
[43] J. A. Aguilar-Saavedra, R. Benbrik, S. Heinemeyer, and M. Perez-Victoria, Phys. Rev. D **88**, 094010 (2013); J. A. Aguilar-Saavedra, EPJ Web Conf. **60**, 16012 (2013).
[44] C. Y. Chen, S. Dawson, and E. Furlan, Phys. Rev. D **96**, 015006 (2017).
[45] A. M. Sirunyan *et al.* (CMS Collaboration), J. High Energy Phys. 11 (2017) 085; 05 (2017) 029; V. Khachatryan *et al.* (CMS Collaboration), Phys. Rev. D **93**, 112009 (2016); G. Aad *et al.* (ATLAS Collaboration), J. High Energy Phys. 02 (2016) 110; Phys. Lett. B **758**, 249 (2016); Eur. Phys. J. C **76**, 442 (2016); J. High Energy Phys. 02 (2016) 110; 08 (2015) 105; Phys. Rev. D **91**, 112011 (2015); V. Khachatryan *et al.* (CMS Collaboration), Phys. Rev. D **93**, 112009 (2016); J. High Energy Phys. 06 (2015) 080; S. Chatrchyan *et al.* (CMS Collaboration), Phys. Rev. Lett. **112**, 171801 (2014); Phys. Lett. B **729**, 149 (2014); G. Aad *et al.* (ATLAS Collaboration), Technical Report No. ATLAS-CONF-2017-015, 2017.
[46] N. Nikiforou (for the ATLAS collaboration), arXiv:1808.04695.
[47] M. Aaboud *et al.* (ATLAS Collaboration), J. High Energy Phys. 08 (2017) 052.
[48] K. Hagiwara, S. Matsumoto, D. Haidt, and C. S. Kim, Z. Phys. C **64**, 559 (1994); **68**, 352(E) (1995).
[49] S. Kanemura, M. Kikuchi, and K. Yagyu, Nucl. Phys. **B907**, 286 (2016).
[50] L. Lavoura and J. P. Silva, Phys. Rev. D **47**, 2046 (1993).
[51] S. Bahrami and M. Frank, Phys. Rev. D **90**, 035017 (2014).
[52] M. E. Machacek and M. T. Vaughn, Nucl. Phys. **B222**, 83 (1983); **B236**, 221 (1984); **B249**, 70 (1985).